MedCrave
Step into the World of Research

Aeronautics and Aerospace Open Access Journal

Research Article

Open Access

CrossMark

N_2O/O_2 blends safe and volumetrically efficient oxidizers for small spacecraft hybrid propulsion

Abstract

A medical grade nitrous oxide and gaseous oxygen fluid blend, "Nytrox," is investigated as significantly safer, but superior performing, alternative for the current generation of environmentally unsustainable spacecraft propellants. In a manner directly analogous to the creation of soda-water using dissolved carbon dioxide, Nytrox is created by bubbling gaseous oxygen under high pressure into nitrous oxide until the solution reaches saturation level. Oxygen in the ullage vapor dilutes the nitrous oxide vapor and increases the required decomposition activation energy of the fluid by several orders of magnitude. Consequently, any risk of inadvertent thermal or catalytic decomposition is virtually eliminated. This paper reports on a preliminary test-and-evaluation campaign where an existing small spacecraft thruster is first tested using gaseous oxygen and 3-D printed ABS as propellants as a baseline. The baseline tests were then repeated using an optimized Nytrox bend as "drop-in" replacement for gaseous oxygen. Test parameters compared include; ignition reliability and required energy, thrust coefficient, characteristic velocity, specific impulse, and fuel regression rate. Nytrox is shown to work effectively and reliably as a replacement for gaseous oxygen, exhibiting a slightly reduced specific impulse and regression rate, but with significantly higher volumetric efficiency. Recommended topics for future research are discussed.

Keywords: hybrid rocket, "Green" propellants, nitrous oxide decomposition, energy of activation, 3-D printing, Nytrox

Volume 3 Issue 4 - 2019

Stephen A Whitmore,[1] Robb L Stoddard[2]

[1]Professor, Mechanical and Aerospace Engineering Department, Utah State University, USA

[2]Graduate Research Associate, Mechanical and Aerospace Engineering Department, Utah State University, USA

Correspondence: Stephen A Whitmore, Professor, Mechanical and Aerospace Engineering Department, Utah State University, Logan, Utah 84321, USA, Tel +01-435-797-2951, Email stephn.whitmore@usu.edu

Received: October 31, 2019 | **Published:** November 20, 2019

Nomenclature

A_c = fuel port cross-sectional area, cm^2

A_{exit} = nozzle exit area, cm^2

A_s = cross sectional area at shock wave position, cm^2

A_1 = venturi inlet area, cm^2

A_2 = venturi outlet area, cm^2

A^* = cross sectional area at which local flow chokes, cm^2

A_{exit}/A^* = nozzle expansion-ratio

C_F = thrust coefficient

C_p = specific heat at constant pressure, *J/kg-K*

C_v = specific heat at constant volume, *J/kg-K*

C_e = effective exhaust velocity, *m/s*

c^* = characteristic velocity of propellants, *m/s*

F = thrust, N

$\bar{G}_{ox}$ = oxidizer massflux, g/cm^2-*s*

$\bar{G}_{total}$ =total massflux, g/cm^2-*s*

g_0 = nominal acceleration of gravity at sea level, *9.8067 m/s*

HVPS = high voltage power supply

I_{sp} = specific impulse, *s*

L_{port} = fuelgrain length, *cm*

$\mathfrak{M}_f$ = mole or volume fraction of one species in a binary gas mixture

M_{exit} = exit plane Mach number

M_w = molecular weight, *g/g-mol*

ΔM_{fuel} = consumed fuel mass, *g*

ΔM_{ox} = consumed oxidizer mass, *g*

$\dot{m}_{fuel}$ = fuel massflow, *g/s*

$\dot{m}_{ox}$ = oxidizer massflow, *g/s*

$\dot{m}_{total}$ = total massflow through the nozzle, *g/s*

O/F = oxidizer/fuel ratio

O/F_{actual} = actual oxidizer-to-fuel ratio

O/F_{stoich} = stoichiometric oxidizer-to-fuel ratio

Nytrox 87 = nitrous oxide, gaseous oxygen solution with 87% nitrous oxide in liquid phase

P_1 = venturi inlet pressure, *psia*

P_2 = venturi throat pressure, *psia*

P_0 = chamber pressure or stagnation pressure, *psia*

p_{exit} = exit plane static pressure, *psia*

p_∞ = ambient pressure, *psia*

R_g = gas constant, *J/kg-K*

R_u = universal gas constant, 8314.4612 *J/kg-K*

r_L = longitudinal average of the fuel port radius, *cm*

r_0 = initial fuel port radius, *cm*

$\dot{r}_L$ = longitudinal mean of fuel regression rate, *cm/s*

$\bar{\dot{r}}$ = mean regression rate over duration of the burn, *cm/s*

s_g = specific gravity

T = venturi flow path temperature, *K*

T_0 = stagnation temperature, *K*

t_{burn} = burn time, *s*

t = generic time symbol, *s*

η^* = combustion efficiency

γ = ratio of specific heats, C_p/C_v

Φ = equivalence ratio

ρ_{fuel} = solid fuel density, g/cm^3

$\rho^* I_{sp}$ = density specific impulse, *N-s/liter*

θ_{exit} = conical nozzle exit angle, *deg*.

Introduction

The Propulsion Research Laboratory (PRL) at Utah State University (USU) recently developed a promising "green" propulsion alternative that has the potential to replace hydrazine for multiple applications. The unique

hybrid propulsion technology derives from the novel electrical breakdown properties of 3-D printed acrylonitrile butadiene styrene (ABS),[1,2] discovered serendipitously while investigating the thermodynamic performance of ABS as a hybrid rocket fuel.[3] This concept has been developed into a power-efficient system that can be started and restarted with a high degree of reliability. Multiple prototype ground-test units with thrust levels varying from 4.5 N to 900 N have been developed and tested.[4,5] Recently, on March 25th, 2018 a flight experiment containing a medium-weight prototype of this thruster system was launched aboard a two-stage Terrier-Improved Malemute sounding rocket from Wallops Flight Facility (WFF). The launch achieved apogee of 172 km, allowing more than 6 minutes in a true space environment above the Von- Karman line. During the mission the USU thruster was successfully fired 5 times in a hard vacuum environment. The payload section was successfully recovered by WFF flight support.

Low resolution telemetry data was successfully downlinked and delivered to USU for analysis. Whitmore & Bulcher[6] report the details of this flight test experiment. Thus, with this spaceflight demonstration the technology readiness level (TRL) of the arc ignition technology must be acknowledged to be at least level 5. In its most mature form this system uses gaseous oxygen (GOX) as the oxidizer with 3-D printed ABS as the fuel. The GOX/ABS propellants resulted in a highly mass efficient system, with a flight weight 25 N thruster system achieving vacuum I_{sp} greater than 300 seconds.[7,8] Unfortunately, unless stored as very high pressures, GOX has a low specific gravity and is a volumetrically inefficient propellant. A higher density alternative is highly desirable. This paper will investigate the potential to use medical grade Nitrous Oxide (N_2O), gaseous oxygen (GOX) blends, typically used for anesthesia or analgesic applications, as "drop-in" replacement for GOX in a legacy small spacecraft thruster system, previously developed and tested at the Utah State Propulsion Research Laboratory. As will be described later in this paper, these mixtures are offered as an alternative to pure N_2O due to an order of magnitude increase in safety and handling, with only a minor decrease in overall performance, and a significant increase in overall volumetric efficiency.

Background on available green propellant options

A recent study[9,10] by the European Space Agency Space Research and Technology Center (ESTEC) has identified two essential design elements to achieving low cost space access and operations; 1) Reduced production, operational, and transport costs due to lower propellant toxicity and explosion hazards, and 2)Reduced costs due to an overall reduction in subsystems complexity and overall systems interface complexity. The ESA/ESTEC study showed the potential for considerable operational cost savings by simplifying propellant ground handling procedures. Developing a non-toxic, stable "green" alternative for most commonly used toxic or potentially-hazardous propellants was highly recommended by the ESTEC study.

Ionic liquid propellants

In response to ESA/ESTEC report and other "becoming green"[11] recommendations, for the past decade the US Air Force (USAF) and the Swedish Space Corporation (SSC) subsidiary *Ecological Advanced Propulsion Systems* (ECAPS) have been pursuing less hazardous alternatives to hydrazine. The two most highly-developed "green-propellant" alternatives are based on aqueous solutions of the *ionic liquids* (ILs) Ammonium Dinitramide (ADN)[12,13] and Hydroxylamine Nitrate (HAN).[14,15] In August 2011, ECAPS announced the results of a year-long series of in-space tests of a 1-N thruster comparing their High Performance Green Propellant (HPGP) to hydrazine on the Prisma spacecraft platform.[16] ECAPS claims that HPGP delivered equivalent–to superior performance, with a specific impulse above 230 seconds. NASA recently selected the USAF-developed HAN-based propellant AF-M315E for its "Green Propellant Infusion Mission (GPIM).[17] In spite of being called "green," by their manufacturers, both of the above-mentioned IL-propellants are toxic to organic tissue, and special handling precautions are required. IL-based propellants are not truly "green." Thus, the USAF has recently begun to refer to such IL-formulations more properly as having "reduced toxicity" properties. In additional to potential toxicity, there exist several key developmental issues associated with IL based propellants that make them unsuitable for small spacecraft applications.

The high water content makes IL-propellants notoriously hard to ignite. Multiple catalyst systems have been developed to augment IL ignitability; however, room temperature ignition does not currently exist. Catalyst beds must be preheated from 350-400ºC before and during ignition, and this preheat can consume up to 15,000 joules of energy. Catalyst beds and associated heating systems add significantly to the inert mass of the spacecraft and the high-wattage preheat requirement presents a significant disadvantage for systems where power budgets are limited. Due to very slow reaction kinetics[8] at moderate pressures (2000-3000 kPa) system latencies associated with IL-based propellants are significant for moderate chamber pressures and may limit the usefulness of IL-propellants for spacecraft maneuvering and control systems.[18] A final major drawback of these propellants is the high combustion temperature that significantly limits the system burn lifetimes. Both the LMP and AFM propellants are prone to uncontrolled energetic events that result in high temperature chemical fires. In spite of this volatility, the performance of ionic

liquid propellants is generally quite low-with vacuum specific impulse values no more than 230 seconds when compared to traditional solid and or bi-propellant options. The combination of these detrimental characteristics compared to their "green" advantages has led some in the industry to question whether Ionic liquids as propellants have been "oversold."[9]

Hybrid rockets as a "green" propulsion alternative

The inherent safety and environmental friendliness of hybrid rocket systems have been known for several decades.[19] Hybrids have the potential to act as an ideal "green" alternative for many of the current generation of toxic or hazardous propellants. Because hybrid systems only require a single fluid flow path, they are of similar complexity to monopropellant systems; but with significantly higher performance. In fact, when properly optimized, hybrid systems have the potential to provide the same performance as significantly more complex bi-propellant liquid systems. While hybrid rocket systems have been considered for applications ranging from large launch systems to nanosatellites, they have not found a real niche with the space-launch and space propulsion industries. Solid and liquid bi-propellant systems have been under development for more than seven decades and the state of technology development for hybrid systems is rather immature by comparison. A low TRL is the primary disadvantage of hybrid systems.

This scenario is analogous to the state of solar electric propulsion (SEP) three decades 153 ago. Systems based on SEP were always considered a higher-risk solution when compared to conventional systems. This situation changed when conventional systems no longer met commercial and/or science-driven requirements, and this technology gap drove the rapid TRL development SEP systems. Technology maturation resulted in the extensive use of arcjet thrusters for GEO communications satellites, eventually resulting in the NSTAR ion systems[20] that set in-space ΔV records on NASA's Deep Space 1[21] and Dawn missions.[22] In similar fashion, as the TRL matures, small hybrid systems offer the potential to fill an unmet and growing need for advanced propulsion both in-space and as launch stages for the emerging SmallSAT market. Hybrid rockets offer particular utility for the upper stages of a nano-launch vehicle. Although a hybrid rocket will increase the overall system dry mass compared to a solid-propellant motor, the capabilities to throttle, shut down on demand, coast, and relight the motor, will offset any loss in performance of the stage. Such a "smart stage" would not only provide ΔV to enable the payload to reach orbit; but can also serve as an on orbit maneuvering system that allows precise placement of the payload. Such a system could also provide extensive capabilities for endo-atmospheric maneuvering for a variety of defense applications.

Hybrid rocket low-power arc-ignition system

Historically, due to the lack of a reliable non-pyrotechnic, multiple-use ignition method, hybrid rockets have never been seriously considered as feasible for in-space propulsion. Hybrid rockets are "safe" due to the relative propellant stability; however, this stability makes hybrid rocket systems notoriously difficult to ignite. The hybrid rocket ignition source must provide sufficient heat to pyrolize the solid fuel grain at the head end of the motor, while simultaneously providing sufficient residual energy to overcome the activation energy of the propellants. Conventional solid-propellant ignition systems use pyrotechnic or "squib" charges to ignite a secondary solid-propellant motor whose high-enthalpy output rate initiates the full motor combustion. Such high-energy devices often come with a suite of environmental and objective risks, and operational challenges. Pyrotechnic charges are extremely susceptible to the Hazards of Electromagnetic Radiation to Ordnance (HERO),[23] and large pyrotechnic charges present a significant explosion hazard that is incompatible with many launch opportunities. Most importantly, for nearly all applications pyrotechnic ignitors are designed as "one-shot" devices that do not allow a multiple restart capability. Thus the great potential for restartable upper stages or in-space maneuvering systems using hybrid propulsion remains largely unrealized. An operational hybrid system with multiple restart capability does not currently exist.

This restartability issue has been overcome by leveraging the unique electrical breakdown properties of certain 3-D printed thermoplastics like acrylonitrile butadiene styrene (ABS).[23] The authors discovered that fused deposition modeling (FDM) processed ABS possesses unique electrical breakdown properties that can be exploited to allow for rapid on-demand ignition. Under normal conditions ABS possesses a very high electrical resistivity and is not considered to be an electrical conductor; however, as FDM-processed ABS is subjected to a moderate electrostatic potential field the layered material structure concentrates minute electrical charges that produce localized arcing between material layers. Joule heating from the resulting arc produces a small but highly-conductive melt layer. This melt layer allows for very strong surface arcing to occur at moderate input voltage levels-between 200 and 300 Volts. Additional Joule heating from the strong surface arcing causes a sufficient fuel material to be vaporized and seeds combustion when simultaneously combined with an oxidizing flow.

Figure 1a shows a typical pyrolysis event, where the ablated hydrocarbon vapor results from inductive arc carving a path across the fuel material. Figure 1b shows a typical 3-D motor head end layout with flow impingement shelves and embedded electrodes. Figure 1c shows typical ignition system electronics schematic.

Shortly after this discovery, the authors of this paper made several unsuccessful attempts to reproduce a similar phenomenon with other hybrid fuel materials including Hydroxyl-Terminated Polybutadiene (HTPB), acrylic, paraffin, and extruded ABS. These experiments also demonstrated that electrical breakdown of FDM-processed ABS occurs at voltages significantly lower than occur with a monolithically fabricated (machined or extruded) article. The extruded or machined ABS does not electrically break down (arc) until voltage levels exceeding 2000 volts are input across the material. This value is roughly an order of magnitude higher than for a similar FDM-processed test article. The observed arcing properties are artifacts of both the grain composite structure due to FDM fabrication and the electromechanical properties of ABS. The associated arc-ignition system, developed by the Utah State University Propulsion Research Laboratory over the past five years, has resulted in a power-efficient ignition system that can be started, stopped, and restarted with a high degree of reliability.[1] A key property of the FDM-printed fuel is an internal structure that enables very low (>3J), rapid onset (>100microsecond), non-catalyzed ignition. The system is entirely impervious to the previously-described hazards associated with electromagnetic radiation (HERO). The low energy ignition process requires a pre-programmed sequence of events that makes inadvertent ignition a virtual impossibility.

[1]Whitmore SA, et al. *Restartable Ignition Devices, Systems, and Methods Thereof*. United States Patent Publication, Pub. No. US 2015/0322892 A1; 2015.

Citation: Whitmore SA, Stoddard RL. N_2O/O_2 blends safe and volumetrically efficient oxidizers for small spacecraft hybrid propulsion. *Aeron Aero Open Access J.* 2019;3(4):171–196. DOI: 10.15406/aaoaj.2019.03.00097

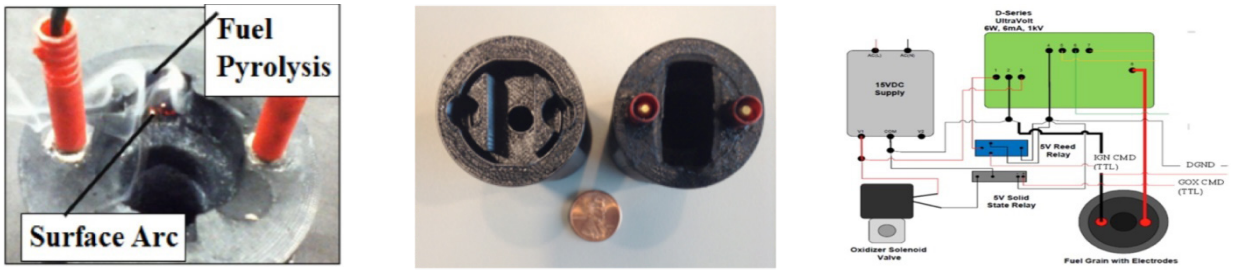

a) Arc-Pyrolys of Fuel *b) Motor Head-end Ignitor Layout* *c) Tyical Arc-Ignition System*

Figure 1 3-D printed hybrid arc-ignition system details.

Choice of non-toxic oxidizers for hybrid 223 space propulsion

Figure 2 shows the available options for hybrid rocket oxidizers. In the practical realm only 4 of these options can be considered as being even reasonably considerable as "green." These are 1) Liquid Oxygen (LOX), 2) Gaseous Oxygen (GOX), 3) Hydrogen Peroxide (H_2O_2), and 4) Nitrous Oxide. (N_2O). Figure 3 compares the relative performances of these oxidizers when burned with a standard industrial formulation of ABS[2] in a hybrid motor. These calculations were performed using the NASA Chemical Equilibrium Program (CEA).[24] Plotted are (a) characteristic velocity c^*, (b) flame temperature, (c) specific gravity, and (d) density velocity ρ^*, which is the product of the mean effective propellant density ρ and c^*. Clearly, using LOX and GOX as oxidizer offers the best mass efficiency c*; with peroxide offering the best volumetric efficiency ρ^*. Unfortunately, LOX which offers both outstanding volumetric and mass efficiency as an oxidizer, must be ruled-out due to the lack of storability.

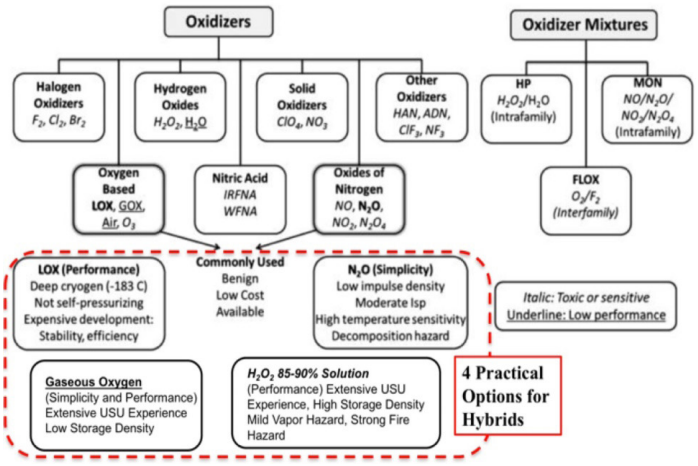

Figure 2 Available options for hybrid oxidizers.[35]

Recent work by the Whitmore et al.,[25,26] (1) and (2), and other organizations[27,28] have adapted hybrid rockets for use with high grade (90%) hydrogen peroxide H_2O_2. Hydrogen peroxide is a very efficient and dense propellant, and makes a good oxidizer. Unfortunately, unless used in very high concentrations (>98%), like IL-based propellants, hydrogen peroxide is notoriously hard to ignite in a hybrid rocket. Most hybrid applications using hydrogen peroxide rely on catalytic ignition, and unfortunately, catalyst development remains a real issue. In all current applications, systems require significant propellant pre-heat and conditioning. None of the existing systems are able to achieve a reliable cold-start. Significant ignition time latencies are experienced. Whitmore[29] reports on the development of a modified version of the previously-described arc ignition system where the injected peroxide stream is thermally decomposed by leading the peroxide flow with a flow of gaseous oxygen that initiates weak combustion of the fuel grain. During this pre-lead event, sufficient heat is released to thermally decompose the injected peroxide stream. The liberated heat and oxygen from decomposition drive full combustion along the length of the fuel grain. Gaseous oxygen pre-leads as small as 500ms reliably initiate combustion. Multiple on-demand relights are provided with this system. Unfortunately, as with the catalytic ignition systems, there exist considerable latency-greater than 1500ms-in order to reach full combustion.

Unfortunately, the significant latencies and pre-requirements make Peroxide an unsuitable oxidizer for in-space applications. Once combustion begins, the performance of the peroxide hybrid systems is quite good with vacuum specific impulse values approaching 300 seconds. Thus, hydrogen peroxide hybrids are more suitable for launch vehicle stages where ignition latencies can be absorbed into the mission timeline, and the high propellant/catbed heating loads can be supplied through available ground power. As described earlier, the low-power arc-ignition system is a key enabling technology for in-space hybrid propulsion. To date, however, the vast majority of development of this system has relied on the use of gaseous oxygen as the oxidizer. Gaseous oxygen is an excellent oxidizer and the proposal team has significant experience with testing of small hybrid thruster systems using GOX. It is entirely "green" and can be quite safely worked with at pressures below 2000 psig, as long as appropriate systems cleanliness standards are adhered-to.[30] Unfortunately, GOX even when stored at high pressure has too low of a density to be practical for long-term space missions requiring even moderate ΔV levels. Thus, by process of elimination the proposers are limited to the use of nitrous oxide as the primary oxidizer for this project. Nitrous Oxide presents a final, reliable alternative for a green hybrid rocket oxidizer for space propulsion. Nitrous oxide is by far the most commonly used hybrid rocket oxidizer. N_2O is an inexpensive and readily available propellant, and has long been considered "standard" oxidizer for hobby-rocket hybrid enthusiasts. Nitrous has the clear advantage of being non-toxic to human tissue and is classified as non-explosive, non-flammable by the US. Occupational Safety and Health Administration (OHSA).[31]

Hazards associated with using nitrous oxide as a rocket propellant

Nitrous Oxide exists as a saturated liquid below its critical temperature of 36.4ºC, and propulsion applications typically must

[2]Stratasys ABSplus-P340.

deal with N_2O in both liquid and vapor form. Although in liquid form N_2O is quite inert and nearly impossible to detonate, in vapor form N_2O can experience a rapid decomposition reaction.[32] This strongly exothermic reaction releases up to 1.864 MJoule per kilogram of material that is decomposed, along with large amounts of nitrogen and oxygen gas. Generally, the decomposition reaction activation energy Ea is large, and the vapor must be heated to temperatures greater than 800ºC in order to induce decomposition of pure N_2O vapor. When a saturated N_2O vapor mixture is contaminated by a small amount of hydrocarbon material, the relative stability of the vapor is lowered and the dissociation activation energy drops dramatically, and decomposition reactions can occur at near room-temperatures for a highly contaminated mixture.[33] In effect the addition of hydrocarbon material to nitrous oxide has the effect of catalyzing or "seeding" the decomposition event. Figure 4 shows the concept, where the activation energy barrier is significantly lowered by the presence of a hydrocarbon contaminant. Because nitrous oxide is a highly polar molecule, it is an exceptionally good solvent and readily picks up and dissolves even minor amounts of hydrocarbon materials that may lie along the flow path. This physical property further exacerbates the potential safety hazards associated with nitrous oxide operations.

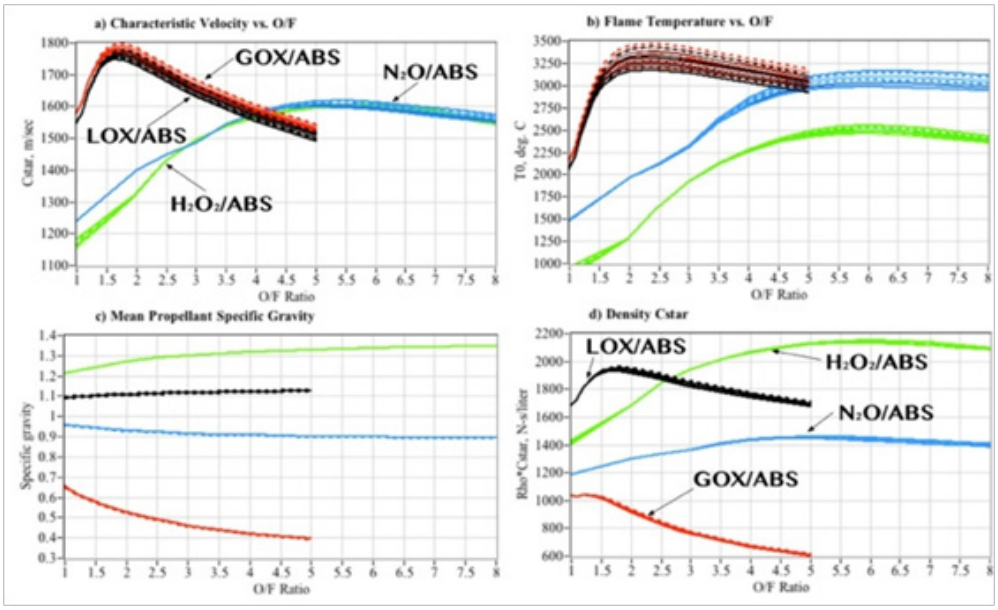

Figure 3 Performance comparison of 4 candidate hybrid oxidizers.

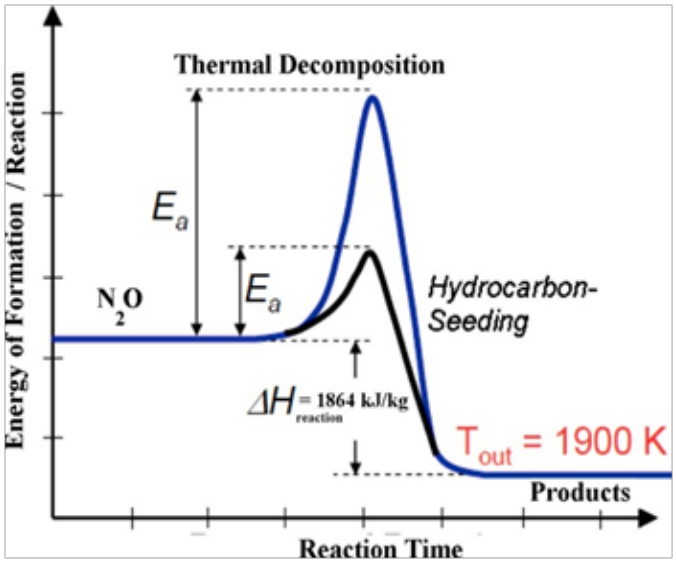

Figure 4 Hydrocarbon seeding of reduces N_2O decomposition activation energy barrier.

The notorious July 26, 2007 Scaled Composites fatal accident[36] in Mojave, CA during Spaceship Two propulsion systems testing, directly resulted from a runway decomposition of contaminated N_2O. The nitrous oxide was stored in an unlined composite tank and effectively acted as a solvent dissolving minor amounts of the composite shell. These "hydrocarbon seeding" contaminants acted as a catalyst to significantly reduce the activation energy for the decomposition reaction. Because the test was being performed during a record heat wave with recorded ground temperatures exceeding 120ºF (49ºC), a significant volume of vapor was being pumped during the ground operations test. It is believed that a small spark from an ungrounded pump provided a small but sufficient quantity of energy to initiate the conflagration. Three people died in the accident.

Even when strict cleanliness standards are adhered-to, the use of pure N_2O as an oxidizer presents a significant hazard for propulsion applications due to the close coupled nature of the oxidizer tank and the combustion chamber. As the motor burns and the N_2O is depleted, a significant volume of ullage vapor will collect in the tank. Tank depletion also implies a significant drop in the internal tank vapor pressure due to adiabatic cooling. This drop in vapor pressure provides the opportunity for a reduced pressure drop across the injector, allowing hot combustion gasses to enter the feed lines and possibly the lower portion of the tank itself. The result is a significant potential for a decomposition reaction, resulting in a fire or explosion.

Citation: Whitmore SA, Stoddard RL. N_2O/O_2 blends safe and volumetrically efficient oxidizers for small spacecraft hybrid propulsion. *Aeron Aero Open Access J.* 2019;3(4):171–196. DOI: 10.15406/aaoaj.2019.03.00097

Mitigation of the N_2O decomposition hazard

Fortunately, it appears that adaptations of procedures developed by the medical and dental anesthesia community offers a strong mitigation to this decomposition hazard.[34] During use of nitrous oxide for anesthesia, a gaseous solution of 50% by volume N_2O and 50% O_2 is administered to the patient. The N_2O content provides the anesthesia properties, while the O_2 content keeps the patient from asphyxiating. In a manner directly analogous to the creation of soda-water using dissolved carbon dioxide; the N_2O/O_2 hybrid solution, referred to as Nytrox, is created by bubbling gaseous oxygen under high pressure into the nitrous oxide until the solution reaches saturation level. Oxygen concentrations as low as 30% can be used for anesthesia applications without encountering issues associated with patient asphyxiation.

Figure 5 plots the vapor/liquid/isotherm diagram for a saturated N_2O/O_2 solution. Figure 5(a) plots the vapor and Figure 5(b) plots the liquid phase mass concentrations of oxygen in solution as a function of saturation pressure. Isotherm curves for temperatures varying from -30ºC to 30ºC are plotted. The 0ºC isotherm is highlighted as the solid blue line for both the liquid and vapor segments of the chart. Reading this diagram, at 0ºC and 86 atmospheres (1250 psig), there exists a "sweet spot" where the concentration of gaseous oxygen in the ullage is a maximum, approximately 37%, while the oxygen fraction in the liquid phase remains relatively low, approximately 13%. Note that the pressure required to hold the O_2 is solution is significantly higher than the natural vapor pressure of N_2O, which is approximately 30 atmospheres at 0ºC. This optimal point allows for the maximum proportion of vapor dilution while maintaining a high density for the liquid fluid. The O_2 in solution provides two immediate safety benefits.

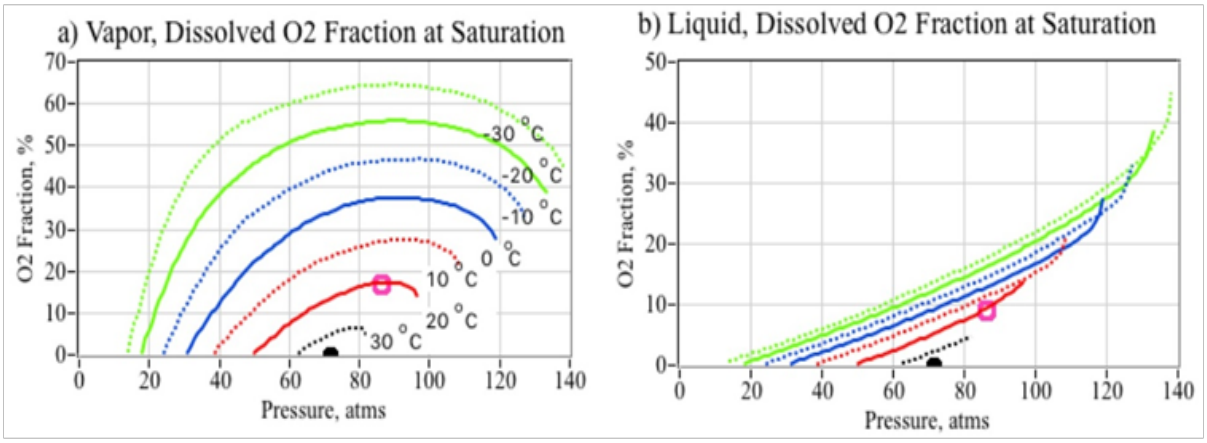

Figure 5 O_2, N_2O solution vapor/liquid isotherm plots.[34]

First, the oxygen mixture in the ullage significantly dilutes the nitrous oxide vapor, and significantly diminishes any potential for a decomposition reaction. Figure 6 plots the minimum energy E_i required for a point source to start a self-sustaining deflagration wave in nitrous oxide with varying initial concentrations of oxygen. For pure nitrous oxide vapor this energy is only about 400-500 miliJoules; however, only a 10% O_2 concentration increases E_i to a value greater than 5 joules, an order of magnitude increase. A 35% O_2 concentration-easily achievable at pressures above 100 atmospheres-increases E_i to greater than 1000 joules, by a factor of more than 4000! In fact, analytical studies performed by Karabeyoglu[35] have demonstrated that blended N_2O/O_2 vapor with at least 20% concentration of O_2 is virtually impossible to ignite using any conceivable ignition Second, the presence of O_2 in the solution significantly increases the "quench diameter," the diameter of a metal pipe that will quench any potential decomposition reaction and ensure that any potential deflagration wave will not propagate. Figure 7 shows this behavior. Note that the quench diameter for pure nitrous oxide is approximately 1.4 cm *(0.6 in)*, and grows to more than 4.5 cm *(1.77 in)* for only 15% O_2 in solution. This difference is a factor of more than 8.7 in terms of the allowable piping cross sectional area. This allowable growth is quite significant in that it allows for substantially higher massflow levels in the system with no increase in deflagration risk.

The key properties associated with using N_2O/O_2 mixtures in lieu of pure N_2O are summarized as

a. Blended Oxidizer systems would be much safer than pure N_2O because vapor phase has large O_2 concentration.

b. Typical system with 30% oxygen in vapor phase requires four to five orders of magnitude larger ignition energy compared with pure N_2O.

c. Safe partial self-pressurization possible at high densities. This property greatly simplifies the design and eliminates the need for a heavy, separate pressurant system using helium or nitrogen.

d. Blended Oxidizer allows improved I_{sp} performance compared with pure N_2O.

e. Critical control variables are temperature and pressure, which determine O_2 mass fraction in liquid and vapor phases.

f. At a given pressure level, Nytrox density higher than GOX by a factor of 3 or 4, and allows for a significant improvement in the overall volumetric efficiency of the propellants.

The calculations of Figure 5 were performed using the Peng-Robinson[36] 2-phase state-equation for binary solutions. The implemented numerical algorithm follows the procedure laid out by Karabeyoglu.[35] The mixing rule used to combine the binary components is based on the model of Zudkevitch & Joffe.[37] For a fluid given temperature, the algorithm searches for the equilibrium pressure level that matches the fugacity of the vapor and liquid phases for each of the binary (O_2, N_2O) fluid components.

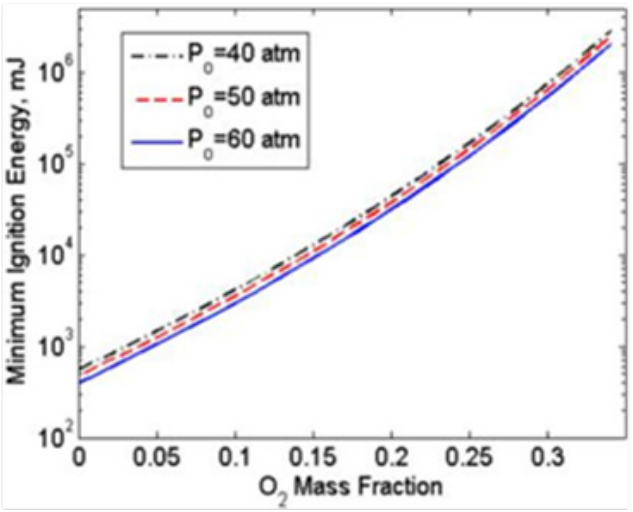

Figure 6 Minimum ignition energy for N_2O/O_2 mixtures at 3 pressure levels.[35]

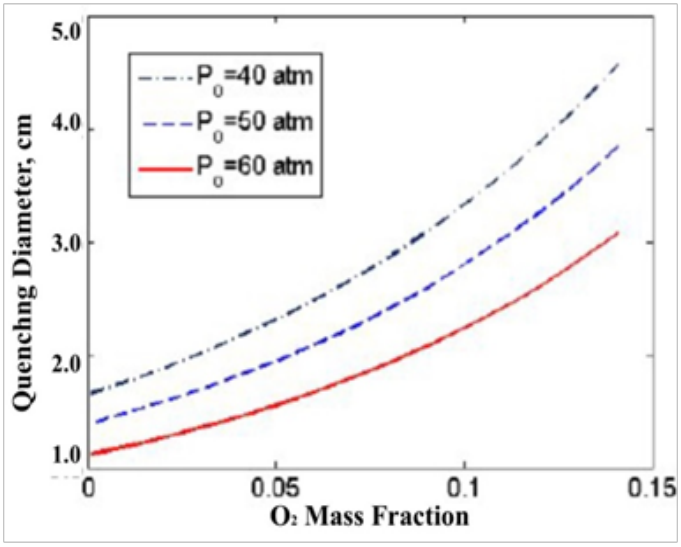

Figure 7 Quenching diameters for N_2O/O_2 mixtures at 3 pressure levels.[35]

Performance of the N_2O/O_2 oxidizer mixtures

Figure 8 plots the densities of the vapor and liquid phases, as calculated by the previously discussed Peng-Robinson model. Referring to Figure 5, at 0ºC a 90% mass concentration of N_2O in the liquid solution corresponds to a vapor pressure of approximately 75 atmospheres (1100 psia). At this vapor pressure the solution density is approximately 800kg/m^3. At a pressure of 120 atmospheres (1470 psia), the percentage of nitrous oxide in the liquid solution drops to only 70% with a corresponding density of only 590kg/m^3. This behavior seems counter-intuitive, but is the nature of two phase binary solutions where the nitrous oxide and oxygen components become mutually dissolved

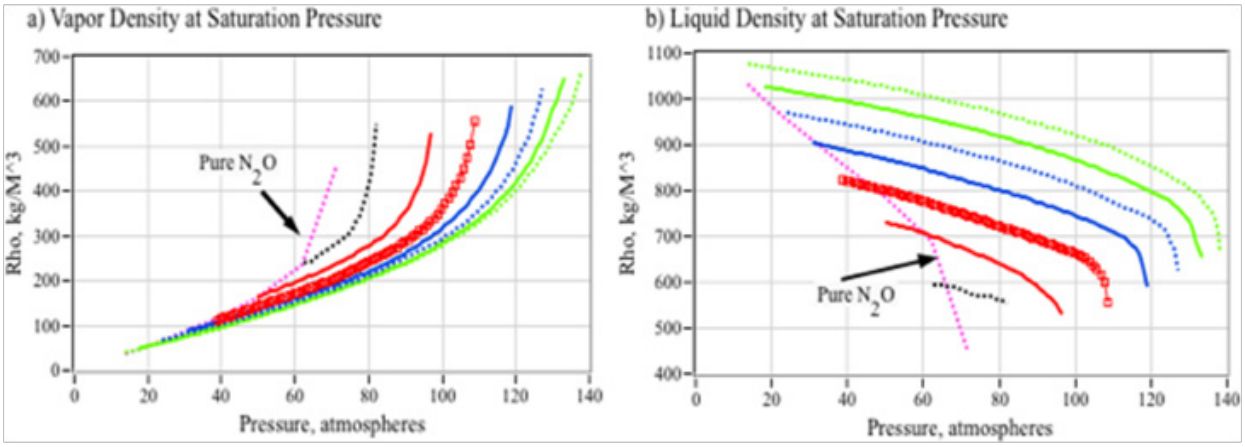

Figure 8 Density of Nytrox vapor and liquid phases at vapor pressure for 6 different isotherms.

Although the solution of O_2 into nitrous oxide slightly reduces the density of the oxidizer, the overall effect includes moderate enhancements of the I_{sp} and a significant reduction of the optimal O/F ratio. This performance-trade makes the N_2O/O_2 solution only slightly less volumetrically efficient than when pure nitrous oxide is used. Figure 9 presents these performance comparisons. Plotted are the (a) characteristic velocity c^*, (b) vacuum I_{sp}, (c) specific gravity, and (d) density I_{sp} ρ^*, which is the product of the mean propellant effective density and the specific impulse. The plotted curves are for 5 different oxidizers when burned with 3-D printed ABS; *GOX*, *pure* N_2O, *90%* N_2O*/10%* O_2, *70%* N_2O*/30%* O_2, and 50% N_2O/50% O_2. For simplicity the Nytrox blends will be referred to by the mass-percentage of nitrous oxide in the fluid blend; respectively, *Nytrox 90*, *Nytrox 70,* and *Nytrox 50*.

The values plotted on Figure 9 were calculated using the CEA program,[24] assuming chamber pressures varying from 100 to 500 psia. The vacuum I_{sp} calculations assume a 40:1 nozzle expansion-ratio. The specific gravity calculation assumes a storage pressure of *1250 psig (86 atms.)*, and fuel density of 1.04g/cm^3. Also plotted on Figures 8(b) and 8(c) are the I_{sp} and ρ^*I_{sp} of Hydrazine. Note that the hybrid mass I_{sp} performance significantly exceeds that of hydrazine. The density performance ρ^*I_{sp} of the *Nytrox 90* solution is greater than hydrazine, whereas the *Nytrox 70* is slightly lower. As expected using GOX as the oxidizer results in the most mass-efficient system, but the low GOX storage density results in the lowest density impulse.

Conversely using pure N_2O gives the best volumetric efficiency, but results in the lowest specific impulse and requires significantly

Citation: Whitmore SA, Stoddard RL. N_2O/O_2 blends safe and volumetrically efficient oxidizers for small spacecraft hybrid propulsion. *Aeron Aero Open Access J.* 2019;3(4):171–196. DOI: 10.15406/aaoaj.2019.03.00097

more oxidizer in order to reach optimal I_{sp}. The curve corresponding to the *Nytrox 90* mixture (at 75 atmospheres vapor pressure) gives the best compromise with a distinct ρ^*I_{sp} optimum occurring at an *O/F* ratio of approximately 4.2. As described previously, increasing the pressure to 84 atmospheres dilutes the nitrous oxide slightly more, but allows the maximum percentage of dissolved oxygen in the vapor phase, and is an important consideration with regard to operational safety.

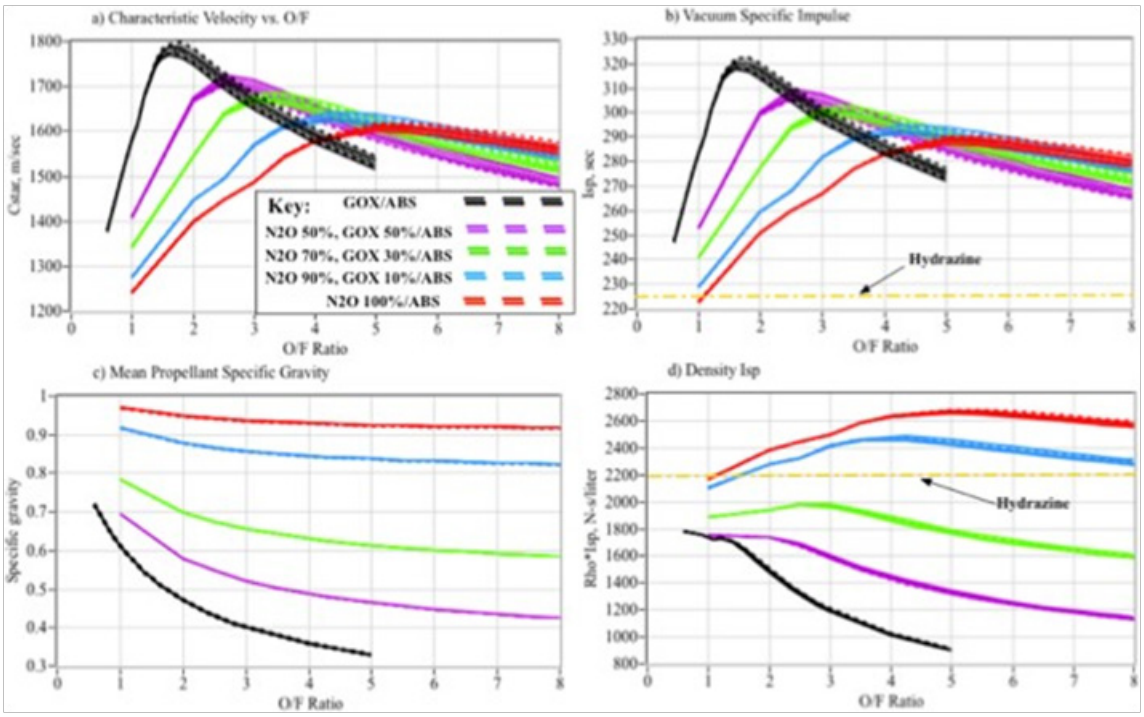

Figure 9 Performance of 3 N_2O/O_2 concentrations compared against pure N_2O and GOX as oxidizer.

Experimental apparatus, instrumentation, and test procedures

This section reports the experimental apparatus and procedures developed for this testing campaign. The hardware details and laboratory procedures for manufacture of the Nytrox solution are presented first. This discussion is followed by description of the test article, experimental apparatus, and procedures used for the hot-fire comparison tests. Because the procedures, established by ad hoc experimentation during this testing campaign are essential to manufacturing the Nytrox mixture with the proper gas proportions, the fill and percolation procedures will be described in detail in the following paragraphs. As a cost-saving measure, many of the test hardware items used were borrowed from previous test articles and adapted for this campaign. The small hybrid thruster used for this test series had previously been optimized for using GOX as the oxidizer; was adapted without change for the Nytrox systems. Due to the preliminary nature of this resting campaign, presented Nytrox results are by no means considered to be optimal.

Nytrox solution processing equipment and fill procedures

For this study highly-purified grades of nitrous oxide and gaseous oxygen were used in order to ensure the resulting Nytrox mixture was free from contaminants and any possible catalytic agents. The gas supplier[3] quotes the N_2O purity at 99.7% by volume; with the primary impurities being traces of oxygen, nitrogen and water vapor. The GOX purity is quoted as 99.4 to 99.7%, with the main impurity being argon. Argon is not liquefiable at normal temperatures, and since argon's critical phase constants are so close to oxygen, its presence is considered negligible with regard to the mixing properties. Also, since argon is inert, there is no potential for catalytic effects.

The basic procedure consists of filling the run tank with the desired weight of N_2O, connecting the filled tank to a GOX supply, and allowing the GOX to bubble up through the liquid nitrous oxide. A dip tube is required on the run tank to allow GOX to percolate up through the liquid phase nitrous oxide without inverting the tank. The dip tube also allows direct delivery of liquid-phase Nytrox for the hot fire tests. During passage through the liquid N_2O, oxygen dissolves into solution and also droplets of nitrous oxide are carried up into thegas phase. The net result is that the volume of liquid in the cylinder steadily diminishes until equilibrium vapor and liquid phase proportions are reached for the fluid temperature. The objective of the developed procedure was to generate a Nytrox solution that possesses a maximum concentration of oxygen in the vapor phase, while maintaining a high N_2O concentration in the liquid phase. As described earlier, and depicted by Figure 5 and Figure 8, at 0ºC this optimum occurs at approximately 86 atmospheres (1250 psig). The result is a "*Nytrox 87*" solution with a vapor phase O_2 concentration

[3]Anon. *Pure Gasses*. Airgas, an Air Liquide Company; 2019. 39-40 p.

Citation: Whitmore SA, Stoddard RL. N_2O/O_2 blends safe and volumetrically efficient oxidizers for small spacecraft hybrid propulsion. *Aeron Aero Open Access J.* 2019;3(4):171–196. DOI: 10.15406/aaoaj.2019.03.00097

of 37%, and a liquid phase O_2 concentration of only 13%. For this equilibrium condition the liquid-phase *Nytrox 87* solution has a density of approximately *0.785g/cm³*. This value is compared to a liquid-phase density of pure N_2O *of 0.907g/cm³* at 0ºC, which is only 15% higher. Using the ideal gas law, GOX at the same temperature and pressure would have a density of only 0.120*g/cm³*, or more than 6.5 times less than dense than the *Nytrox 87* solution.

Nytrox tank fill apparatus and fill procedure

The high grade N_2O is delivered in a K-size tank. The GOX-supply also comes delivered in a K-size tank with an internal pressure of 2000 psig. To ensure safety during the Nytrox mixing procedure, the pipes and fittings as procured were exclusively rated for Nitrous Oxide service. Also, all personnel present during the mixing process wore the proper safety equipment. The Nytrox was mixed in a commercial *NOS*® tank with a 10-lbm fill capacity, and designed for automotive applications.[4] This particular unit comes with a pre-installed dip tube, has a design burst pressure of 8000 psig and a factory installed burst disc rated to 3000 psig. Safety of using this tank was verified since the pressures desired were well below the burst disc pressure. All service lines were fabricated from braided stainless steel, and are specifically rated for nitrous oxide service. To begin the Nytrox manufacturing procedure, the NOS run tank is first filled with the desired amount of liquid nitrous oxide, typically 5-7 lbs. (1100-1,550 grams). To protect all personnel in the advent of an unlikely decomposition event, the N_2O fill procedure is performed in a wire cage. Figure 10 shows the NOS run tank fill apparatus. The NOS run tank was placed in an ice bath to lower the tank temperature to 0ºC, while the N_2O K-service tank was kept at room temperature. The temperature difference created by the ice bath lowers the vapor of the fluid in the NOS run tank, creating a pressure difference that initiates in fluid flow. After ensuring that the needle valve and both tanks are closed.

An electronic scale with serial output is used to measure the nitrous oxide mass moved from the service tank to the run tank. Before filling the empty tank, weight was recorded, and the scale was tared. The NOS run tank/ice bath combo is then placed on a scale used to measure the weight of N_2O added to the tank. With the needle valve closed, both the N_2O tank and the NOS run tank were opened. The needle valve was then opened slowly to allow flow of N_2O into the NOS run tank at a slow rate. Once the scale display reads the desired mass, the needle valve was closed, followed by the N_2O service tank and NOS run tank valves. Slowly disconnecting the fill line from each bottle allows lines to vent during removal.

Nytrox/O2 percolation procedure

All gas-mixing procedures were performed in the *Battery Limits and Survivability Testing* (Blast) Lab, USU's on campus jet engine and rocket test facility. This service bunker has 1-foot thick concrete walls with two 6" thick Plexiglas viewing pane from which test conductors can view hazardous operations directly in an indoors shirt-sleeve environment. Conveniently the Blast lab is located directly across the street from the PRL facility. Figure 11 shows the physical layout of the assembled system (a), and (b) shows the percolation apparatus block diagram. Two different service lines are used for mixing the Nytrox. The fill line from the N_2O to the NOS run tank was approximately 8 ft. long consisting of the following components: four 2 ft. line sections, one N_2O filter to ensure cleanliness of N_2O, one backflow prevention (check) valve rated at 3000 493 psig, and one precision flow-adjustment (needle) valve rated at 2000 psig. The fill line from the O_2 to the NOS run tank was approximately 4 ft. long consisting of the following components: two 2 ft. line sections, one backflow prevention (check) valve rated at 3000 psig, a precision flow-adjustment (needle) valve rated at 2000 psig, and a pressure regulator rated at 3000 psig.

Figure 10 N_2O fill apparatus.

After ensuring that the needle valve and both tanks are closed, the O_2 fill line is attached to both the O_2 tank and the NOS run tank with the check valve allowing flow into the NOS run tank. The O_2 tank is then opened and the pressure regulator is set to a downstream pressure of 1250 psig. The NOS run tank is then opened. Since a very slow flow of O_2 is desired into the NOS run tank, the needle valve is opened just until O_2 flow can be heard. This configuration is then left to allow the O_2 to percolate through the N_2O currently in the NOS run tank and reach pressure equilibrium. Once pressure equilibrium is reached and the pressure in the NOS run tank is confirmed and the needle valve and both tanks are closed. As before, the service lines are slowly disconnected from each bottle allowing the line to vent during removal. Once the NOS run tank is filled, a final mass is logged before storing the Nytrox for future testing. To further mitigate any potential risk of runaway decomposition reaction, the serviced NOS run tank is stored potable in a freezer unit to keep vapor pressures low and ensure a minimal amount of N_2O vapor in the tank ullage. By decreasing the temperature of the NOS run tank, the activation energy barrier is raised even further to prevent any accident from occurring. Internal freezer temperatures are kept around –10ºC.

Hot fire test apparatus and instrumentation

This section details the hardware, instrumentation and test procedures used to perform the hot fire evaluation tests. The hot fire testing campaign was performed using the previously-described Blast Lab test cell. Whitmore and Bulcher[7] and Whitmore[8] describe the

[4]Anon. *NOS 10lb Super Hi-Flow Nitrous Bottle Kit*. Holley Inc.; 2019.

analytical methods, test apparatus, instrumentation, test procedures, and analysis methods used to derive the presented data in much fuller detail. This section summarizes the major conclusions of this testing campaign.

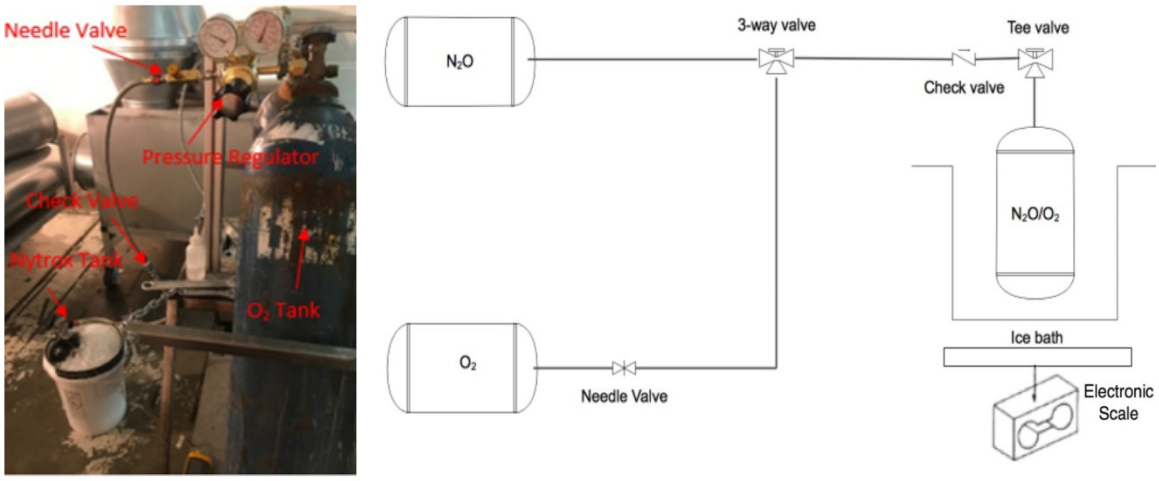

a) Physical Layout

Figure 11 Nytrox percolation apparatus.

Thrust chamber

The legacy GOX/ABS small spacecraft thruster of Refs.[7,8] was adapted for use in the testing campaign. Figure 12 presents the details of the thrust chamber assembly. Figure 12(a) presents a 2-D schematic. Figure 12(b) presents a photograph of the disassembled system. Depicted are the major components; i) graphite nozzle, ii) nozzle retention cap, iii) motor case, iv) 3D printed fuel grain with embedded electrodes, v) insulating phenolic liner, vi) chamber pressure fitting, and vii) single-port injector cap. The 38-mm diameter thrust chamber is constructed from 6061-T6 high-temperature aluminum, and was procured commercially from Cesaroni Inc.[5] Table 1 summarizes the thruster geometry and other specifications. The electronic arc-ignition system for this thruster was described previously and is depicted by Figure 1.

Hot fire thrust stand apparatus and instrumentation

Figure 13 shows the flight weight motor assembled (a) and mounted to the test load balance, (b) shows the piping and instrumentation diagram (P&ID) of the test systems. Test stand measurements include venturi-based

GOX massflow measurements, load-cell based thrust measurements, chamber pressure, and multiple temperature readings at various points along the flow path. The differential venturi pressure transducer was installed to increase the accuracy of the sensed pressure drops. The thrust-stand support members allow bending along the direction of thrust to prevent them from interfering with the measured load. The entire test assembly is made using commercially available T-slot[6] extruded-aluminum components. Figure 14 shows the instrumentation deck layout. On the top of the instrumentation deck there are three NI DAQ units shown; (left to right) USB 6009, USB 6002, USB 9213. The NI USB 6002 is used to read and write data from several bridge transducers and acts as the controller for thehigh voltage signal using a single TTL-level (3.2-volt) digital command. The NI USB 6009 served as an additional device to read and write data since all the channels on the USB 6009 were used. The NI USB 9213 served as a read and write device for the thermocouple probe inserted in the flow to record the temperature of the Nytrox. All data acquisition and control processes were programmed onto a control laptop computer using the LabVIEW® programming language. Communication from the laptop to the instrumentation system was achieved by using a 30-ft amplified USB 2.0 extension cable.

The ignition system power processing unit (PPU) is based on the UltraVolt® D-series line of high-voltage power supplies (HVPS).[7] As previously pictured in Figure 1, the HVPS provides the inductive ignition spark that pyrolyzes sufficient ABS material to seed combustion. The D-series HVPS units take a 15-volt DC input and provide a current-limited (7.5 mA) high voltage output-up to 1000 V or 6 Watts total output. Previous experience with this ignition system has demonstrated that ignition can be reliably achieved using as little as 3 watts. Depending on the impedance on the arc path between the ignitor electrodes, the dissipated voltage typically varies between 10 and 400 volts. Total energy of ignition is typically less than 3 Joules. Ignition energy results will be reported later in this paper.

Directly aft of the thrust chamber lies the solenoid actuated GOX run-valve. The solenoid flow valve is actuated via a digital out command from the instrumentation. The National Instruments USB-6002 initiates "Ignition Control" sending power to the solenoid valve via the solid-state relay and HVPS TTL-level activate signal using the NI 6002 as the controller. The 24V power supply is used to supply power to the solenoid valve and HVPS; whereas, the 15V power supply is used to power the transducers. The thermocouples, venturi inlet, differential, and chamber pressure transducers, along with the load cell all have their signals conditioned using National Instruments Data Acquisition (DAQ) units.

Hot fire test procedures

Initially a set of baseline tests was performed using gaseous oxygen as the oxidizer. This test series will ensure that the system has

[5]Anon. *Cesaroni Pro-X, A Better Way to Fly*. Pro38® hardware.
[6]Anon. T-Slotted Aluminum Extrusions; 2016.
[7]Anon. *High Power 8C-30C Series, Single Output High Voltage DC/DC Modules*. UltraVolt, Inc., 2016.

been returned to the status that existed during the testing campaign of Ref.[7] Key parameters to be measured during this baseline test series include ignition power, thrust, chamber pressure, massflow, fuel regression rate, and specific impulse. Following the baseline tests, the GOX tank was swapped for the NOS run tank filled with the processed Nytrox. Other than the change in oxidizer, the test assembly will remain identical. For the Nytrox tests, the downstream regulator setting is adjusted to de liver this blended mix at exactly the same chamber pressure as for the GOX tests. Special attention was placed on establishing the required ignition power, and the resulting thrust, specific impulse and fuel regression rates. Tests were performed using the NOS run tank at room temperature; and also with the tank chilled by an Ice-bath to ensure that liquid solution is injected into the motor.

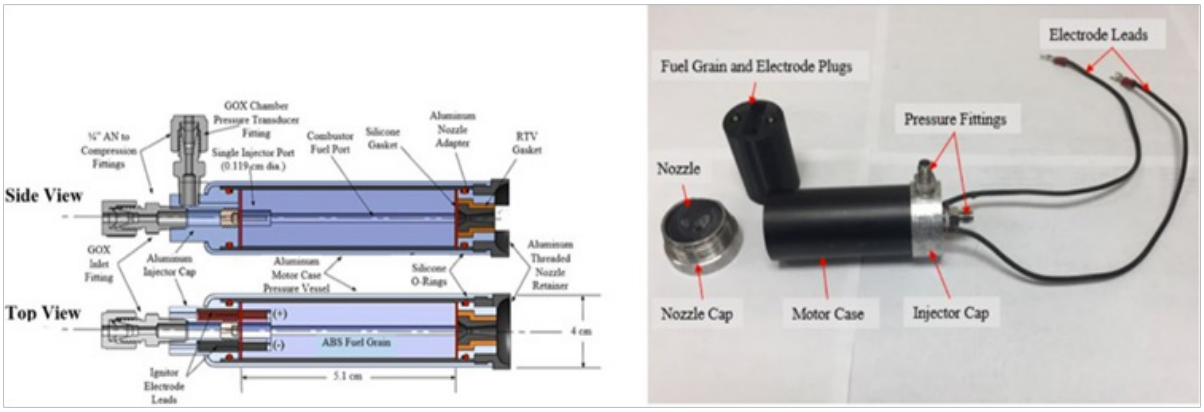

(a) 2-D Schematic (b) Thrust Chamber Components

Figure 12 Test article thruster assembly.

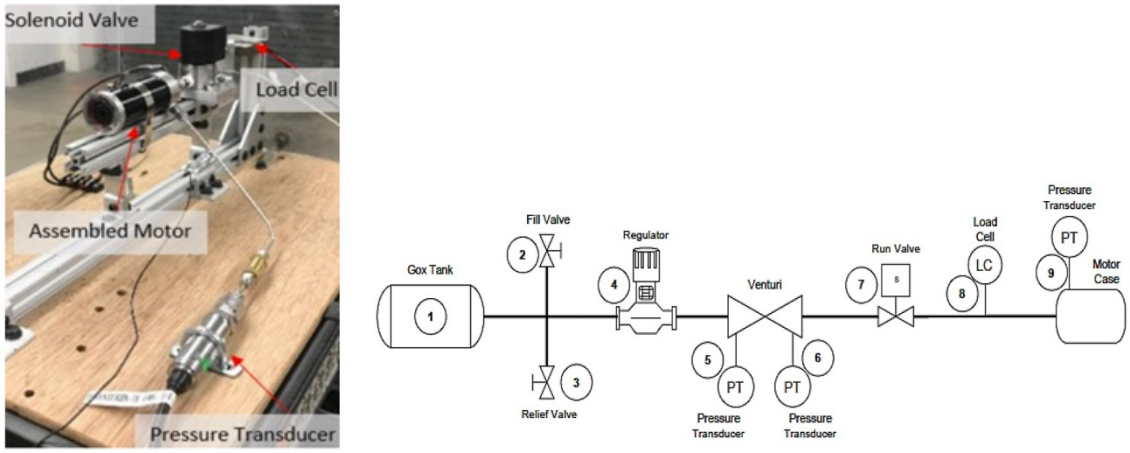

a) Mounted to Test b) Piping and Instrumentation

Figure 13 Thruster systems test apparatus.

The procedures followed were the same for both GOX baseline and Nytrox Tests. Before the motor was assembled, the fuel grain weight and port diameters at both the top and bottom were recorded. The nozzle throat and exit plane diameters were also logged. Finally, the NOS run tank weight and pressure were logged. Once the pre-test measurements were recorded the motor was assembled. The motor assembly leads were connected to the cart, oxidizer feed line attached, and motor assembly mounted to the test stand. The test stand was then moved to the Blast Lab test area for testing. Inside of the test area, A/C power was then connected to the test stand and connectivity checked using the designated lab test computer. The feed line from either the GOX or the NOS run tank was attached to the thruster systems. The entire feed line was then leak checked to ensure proper connections, and the regulator for the oxidizer feed pressure was set to 310 psig.

For this test campaign power to the ignition "spark" power was active for a total of two seconds, pre-leading the opening of the oxidizer run valve by 1 second. The oxidizer run valve was pre-programmed to open for a prescribed amount time, and for these tests this time varied from 1 second to more than 4 seconds. The motor would snuff immediately after closure of the run valve. Typically, one fuel grain allows for 8 seconds of burn time, so a typical test series would allow four tests of 2 seconds each on a single fuel grain. Following each burn, the previously described weight and geometry measurements were repeated and logged.

Analytical methods

Computational sequence for calculating the GOX massflow

For the GOX mass flow sensor, the massflow calculation was rather straight forward, and the compressible venturi massflow equations are derived from material presented by Anderson.[38] The

entering stagnation pressure is calculated from the sensed inlet P_1 and throat P_2 absolute pressure levels, and the venturi inlet A_1 and throat flow areas A_2

$$P_0 = \left[\frac{\left(\frac{A_1}{A_2}\right)^2 \cdot \left(P_1\right)^{\frac{\gamma+1}{\gamma}} - \left(P_2\right)^{\frac{\gamma+1}{\gamma}}}{\left(\frac{A_1}{A_2}\right)^2 \cdot \left(P_1\right)^{\frac{2}{\gamma}} - \left(P_2\right)^{\frac{2}{\gamma}}} \right] \tag{1}$$

Once the true inlet stagnation pressure is calculated, then the achieved massflow is calculated using the unchoked compressible massflow equation

$$\dot{m}_{ox} = C_d \cdot A_1 \cdot P_0 \sqrt{\left(\frac{2\gamma}{\gamma-1}\right)\frac{1}{Rg \cdot T}\left[\left(\frac{P_1}{P_0}\right)^{\frac{2}{\gamma}} - \left(\frac{P_1}{P_0}\right)^{\frac{\gamma+1}{\gamma}}\right]} \tag{2}$$

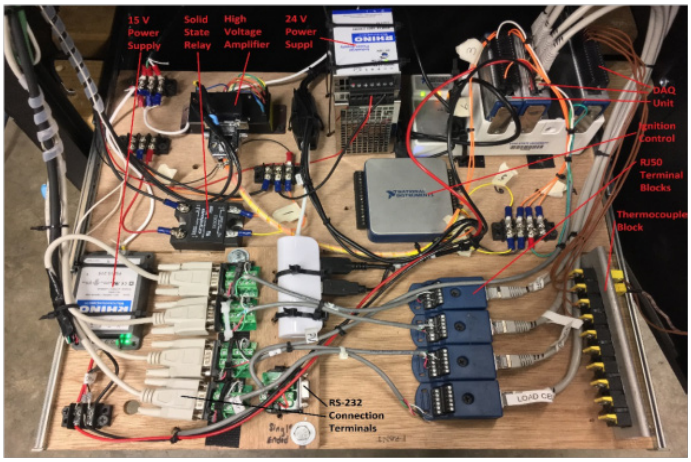

Figure 14 Instrumentation deck layout.

The calculation of Eq. (2) requires a temperature measurement T, and this value was measured using a thermocouple installed on the venturi flow block. The flow discharge coefficient C_d accounts for frictional flow losses. Both venturi flow meters were calibrated using cold flow tests that captured the total mass passed through the system. Previously Refs.,[7,8] performed extensive cold flow tests and measured the discharge coefficient for GOX flow to be approximately 0.95. Since the test setup for the GOX baseline tests did not change from the original tests of Refs.,[7,8] the Venturi was not calibrated using cold GOX flow for this campaign.

Computational sequence for calculating the Nytrox massflow

In contrast to the GOX flow, due to the two-phase, binary fluid nature of the Nytrox solution flow, deriving meaningful massflow measurements from the venturi sensor is rather more complicated. Multiple models have been previously developed for two phase nitrous oxide mass flows. These include models developed by Zilliac and Karabeyoglu,[39] Dyer,[40] Whitmore & Chandler,[41] Zimmerman et al.,[42] and Waxman et al.[43] It is likely that these models, each developed for the flow of a single saturated liquid are applicable to the two phase binary fluid injector problem, but a solid theoretical foundation for this adaptation has yet to be developed. Thus, for this preliminary proof-of-concept testing campaign, the Nytrox massflow through the venturi was modeled as a simple compressible gas flow with a calibrated discharge coefficient. Here, an ideal gas is assumed with the gas properties derived from vapor phase mole fraction as calculated by the Peng-Robinson model.[36] The associated ideal gas thermodynamic properties are

a. Molecular weight,

$$M_{w_{Nytrox}} = \mathfrak{M}_{f_{N_2O}} \cdot M_{w_{N_2O}} + \mathfrak{M}_{f_{O_2}} \cdot M_{w_{O_2}} \tag{3}$$

b. Gas Constant,

$$R_{g_{Nytrox}} = \frac{R_u}{M_{w_{Nytrox}}} \tag{4}$$

c. Specific Heat at Constant Pressure,

$$C_{p_{Nytrox}} = \frac{\mathfrak{M}_{f_{N_2O}} \cdot M_{w_{N_2O}} C_{p_{N_2O}} + \mathfrak{M}_{f_{O_2}} \cdot M_{w_{O_2}} \cdot M_{w_{O_2}}}{M_{w_{Nytrox}}} \tag{5}$$

d. Ratio of Specific Heats

$$\gamma_{Nytox} = \frac{C_{pNytrox}}{C_{v_{Nytrox}}} = \frac{C_{pNytrox}}{C_{pNytrox} - R_{g_{Nytrox}}} \tag{6}$$

In Eqs (3)-(6) the symbol M_f represents the mole fraction of a given vapor species and R_u represents the universal gas constant. Using these values for R_g and γ, the Nytrox massflow is calculated using Eqs. (1) and (2)

Computational sequence for fuel regression rates, instantaneous O/F, and equivalence ratios

Although the inline venturi measures the oxidizer mass flow in real-time, the test stand could not measure real-time fuel mass flow. Thus, for this testing campaign the "instantaneous" fuel mass flow rates were calculated as he difference between the measured nozzle exit and oxidizer mass flow rates,

$$\dot{m}_{fuel} = \dot{m}_{total} - \dot{m}_{ox} \tag{7}$$

For all runs the regulator pressure and injector port diameter were pre-set to choke the injector flow and ensure a constant oxidizer mass flow. Choking the injector flow ensured very low run-to-run variability in the oxidizer massflow rate, and significantly reduced the risk of incurring injector-feed coupling instabilities during combustion. The nozzle exit mass flow time history was calculated from the measured chamber pressure time history P_0, nozzle throat area A^*, and the exhaust gas properties (flame temperature T_0, ratio of specific heat γ, molecular weight M_w, and specific gas constant R_g) using the 1-dimensional choking mass flow equation, (Anderson [38], Chapter 4).

$$\dot{m}_{total} = A^* \cdot P_0 \cdot \sqrt{\frac{\gamma}{R_g \cdot T_0} \cdot \left(\frac{2}{\gamma+1}\right)^{\frac{\gamma+1}{(\gamma-1)}}} \tag{8}$$

The mean longitudinal fuel regression rate was calculated from the fuel mass flow by,

$$\dot{r}_L = \frac{\dot{m}_{fuel}}{2\pi \cdot \rho_{fuel} \cdot r_L \cdot L} \tag{9}$$

Integrating Eq. (9) from the initial condition to the burn time frames solves for instantaneous mean port radius,

$$r_L(t) = \sqrt{r_0^2 + \frac{1}{\pi \cdot \rho_{fuel} \cdot L}\int_0^t \dot{m}_{fuel} dt} \tag{10}$$

Citation: Whitmore SA, Stoddard RL. N_2O/O_2 blends safe and volumetrically efficient oxidizers for small spacecraft hybrid propulsion. *Aeron Aero Open Access J.* 2019;3(4):171–196. DOI: 10.15406/aaoaj.2019.03.00097

The terminal cross sectional area of the fuel port is,

$$A_c\left(t_{burn}\right) = \pi \cdot r_0^2 + \frac{\Delta M_{fuel}}{\rho_{fuel} \cdot L_{port}} \tag{11}$$

The mean fuel regression rate over the duration of the burn is calculated by

$$\overline{\dot{r}} = \frac{\Delta M_{fuel}}{\pi \cdot \rho_{fuel} \cdot L_{port} \cdot \left(r_{t_{burn}} + r_0\right) \cdot t_{burn}} \tag{12}$$

The mean oxidizer mass flux, total mass flux, O/F ratio, and equivalence ratio are estimated by

$$\begin{bmatrix} \overline{G}_{ox} = \dfrac{\int_0^{t_{burn}} \dot{m}_{ox}(t).dt}{A_c\left(t_{burn}\right)} \\ \overline{G}_{ox} = \dfrac{\Delta M_{fuel}}{A_c\left(t_{burn}\right)} \\ O/F = \dfrac{\int_0^{t_{burn}} \dot{m}_{ox}(t).dt}{\Delta M_{fuel}} \\ \Phi = \dfrac{O/F_{stoich}}{O/F_{actual}} \end{bmatrix} \tag{13}$$

For each data point in the burn time history, two-dimensional tables of thermodynamic and transport properties were interpolated to calculate the gas constant R_g, ratio of specific heats γ, and flame temperature T_0. The table of equilibrium properties of the GOX/ABS exhaust plume were developed by Ref.[3] with measured chamber pressure P_0, combustion efficiency η^*, and mean O/F ratio as independent look up variables for the tables. Reference[3] used NASA's industry standard chemical equilibrium code CEA code[24] to perform the calculations. Each fuel grain was burned multiple times to allow interim fuel mass consumption measurements between burns. The corresponding oxidizer mass consumed was calculated by integrating the venturi mass flow time history over the burn duration. The mean O/F ratio over the burn duration was estimated by dividing the consumed oxidizer mass by the consumed fuel mass. By adjusting η^* the flame temperature was scaled

$$T_{0_{actual}} = \eta^{*2} \cdot T_{0i_{deal}} \tag{14}$$

To adjust nozzle-exit massflow and the resulting consumed fuel massflow,

$$\Delta M_{fuel} = \int_0^t \left(\dot{m}_{total} - \dot{m}_{ox}\right) dt \tag{15}$$

Adjusting input combustion efficiency upwards has the effect of increasing the calculated fuel mass consumption, and downwards decreases the calculated fuel mass consumption. The fuel massflow calculation starts with an assumed combustion efficiency of $\eta^* = 0.90$. The calculations of Equations (3-10) were iterated, adjusting η^* until the calculated fuel mass equals the measured mass and total consumed propellant O/F ($\Delta M_{ox}/\Delta M_{fuel}$) within a prescribed level of accuracy (0.5 %).

Table 1 Motor geometry and parameter specifications

Parameter	**Injector**		**Single Port, 0.127 cm (0.05 in.) Diameter**	
Fuel Grain	Diameter: 3.168 cm (1.246 in.)	Length: 6.850 cm (2.70 in.)	Initial Weight: 50.0 g Print Density: 0.955 g/cm^3	Initial Port Diameter: 0.625 cm (0.246 in.)
Motor Case	Diameter: 3.8 cm (1.50 in.)	Length: 13.8 cm (5.43 in.)	Wall Thickness: 1.5 mm (0.059 in.)	
Conical Graphite Nozzle	Initial Throat Diameter: 0.375 cm (0.148 in.)	Exit Diameter: 0.577 cm (0.277 in.)	Ambient Tests Initial Expansion-ratio: 2.07:1	Nozzle Exit Angle: 5.0 deg.

Once the total mass flow and combustion chamber properties were calculated as described above, the 1-dimensional de Laval flow equations (Anderson [38], Chapter 4) were used to calculate the exit plane Mach number, pressure, effective exhaust velocity, thrust, thrust coefficient, specific impulse, and characteristic velocity. The following flow sequence was used for the de Laval flow model

a. Numerical Solution for Exit Plane Mach Number,

$$\frac{A_{exit}}{A^*} = \frac{1}{M_{exit}}\left[\left(\frac{2}{\gamma+1}\right)\left(1 + \frac{\gamma-1}{2}M_{exit}^2\right)\right]^{\frac{\gamma+1}{2(\gamma-1)}} \tag{16}$$

b. Exit Plane Static Pressure,

$$p_{exit} = \frac{P_0}{\left(1 + \frac{\gamma-1}{2}M_{exit}^2\right)^{\frac{\gamma}{\gamma-1}}} \tag{17}$$

c. Effective Exhaust Velocity,

$$C_e = \lambda_{exit} \cdot M_{exit} \cdot \sqrt{\frac{\gamma \cdot R_g \cdot T_0}{1 + \frac{\gamma-1}{2}M_{exit}^2}} + \frac{\left(p_{exit} - p_\infty\right) \cdot A_{exit}}{\dot{m}_{total}} \tag{18}$$

d. Thrust and Thrust Coefficient,

$$F = \dot{m}_{total} \cdot C_e \tag{19}$$

$$C_F = \frac{F}{P_0 \cdot A^*} \tag{20}$$

e. Finally, Specific Impulse, Characteristic Velocity, and Density Specific Impulse

$$I_{sp} = g_0 \cdot C_e \tag{21}$$

$$c^* = \frac{P_0 \cdot A^*}{\dot{m}_{total}} \tag{22}$$

$$\rho^* I_{sp} = S_g \cdot g_0 \cdot I_{sp} \tag{23}$$

Citation: Whitmore SA, Stoddard RL. N_2O/O_2 blends safe and volumetrically efficient oxidizers for small spacecraft hybrid propulsion. *Aeron Aero Open Access J.* 2019;3(4):171–196. DOI: 10.15406/aaoaj.2019.03.00097

In Eq. (18) $\lambda_{exit} = 1/2\left(1+\cos\left(\theta_{exit}\right)\right)$, where λ_{exit} is the momentum thrust correction factor and θ_{exit} is the conical nozzle exit angle. In Eq. (21) g_0 is the normal acceleration of gravity at sea level, *9.8067 m/s²*. For the $\rho * I_{sp}$ calculation, s_g is the mean effective specific gravity of the propellants, and is calculated as

$$S_g = \frac{S_{g_{ox}} \cdot O/F + S_{g\,fuel}}{O/F + 1} \tag{24}$$

In Eq. (24) the parameter refers to the storage specific gravity of the oxidizer and not the downstream specific gravity. The thrust coefficient C_F and specific impulse I_{sp} were also calculated from the thrust values sensed by the test stand load cell. The values calculated by Eqs. (20) and (21) provide redundant measures, and will be presented later in order to support the verisimilitude of the collected test data.

Results and discussion

The results of the previously described testing campaign are presented in this section. The properties of the resulting Nytrox solution are described first, followed by the test results from the 2-Phase Nytrox venturi calibration. Finally, the results from sixteen successful tests are presented. Of those tests, 6 hot-fire burns used GOX as the oxidizer, and 10 hot fire burns swapped out Nytrox for GOX. The GOX results established the system baseline. Results from the GOX and Nytrox burn tests will be presented individually and then compared. Table 2 summarizes the Nytrox processing results.

Table 2 Nytrox mix batch specifications

Nytrox batch No.	NOS tank tare weight	NOS tank internal volume	Final tank fill pressure	Final tank fill temperature	Final filled tank weight	
1	7.657 kg	6.846 liters	1250 psig (8704.4 kPa abs)	0°C	10.524 kg	
2	7.657 kg	6.846 liters	1270 psig (8842.3 kPa abs)	0°C	10.578 kg	
	Oxidizer added	**Mean oxidizer density**	**N_2O added to tank**	**O_2 added to tank**	**Total O_2 mass fraction, %**	
1	2.867 kg	0.419 g/cm³	2.234kg (4.924 lb)	0.633 kg	22.10%	
2	2.921 kg	0.427 g/cm³	2.267kg(4.996 lb)	0.654 kg	22.40%	
	Liquid density (Peng-Robinson)	**Vapor density (Peng-Robinson)**	**Liquid O_2 mass fraction**	**Vapor O_2 mass fraction**	**Liquid Mol. Wght.**	**Vapor Mol. Wght.**
1	0.785 g/cm³	0.241 g/cm³	12.63%	37.14%	42.02 g/mol.	38.63 g/mol.
2	0.782 g/cm³	0.247 g/cm³	12.63%	37.14%	41.97 g/mol.	38.62 g/mol.
	Mass of liquid in tank	**Mass of vapor in tank**	**Volume of liquid in tank**	**Ullage volume in tank**	**Mix quality in tank**	
1	1.757 kg	1.110 kg	2.238 liters	4.608 liters	0.387	
2	1.799	1.122	2.302 liters	4.544 liters	0.384	

Making the Nytrox mixture

The procedures described by Section H were followed to generate the Nytrox batches used for this testing campaign. For each batch the *NOS* run tank was filled with *5 lb. (2.27 kg)* of nitrous oxide, and allowed to chill in the ice bath. A *5 lb*. fill is 1/2 of the rated fill capacity for NOS run tank. Once the tank temperature stabilized at *0ºC*, the O_2 needle valve was opened and oxygen was allowed to percolate through the system. Once connected with the regulator set at 1250 psig, the process takes about 2 hours to reach equilibrium. At the time of this publication, two complete batches of Nytrox have been processed. The batch comparisons are remarkably similar. Batch 1 reached an equilibrium pressure of 1250 psig, with batch 2 reaching an equilibrium pressure of 1270 psig. Batch 2 ended up with slightly more oxidizer in the fill 2.921 kg as compared to 2.891 for batch 1. However, the intensive fluid properties were remarkably similar, with the effective fill densities for batch 1 and batch 2 being *0.419* and *0.427 g/cm³* respectively. This difference is of less than 1%. Thus, the established fill procedures were quite successful and worked as well as planned.

Nytrox venturi calibration

As described in the previous section, the flow pf the two-phase, binary N_2O/O_2 fluid mixture through the venturi flow meter is quite complex and a first-principle flow mode has not yet been developed. Thus, a simple calibration procedure was performed in order to measure the discharge coefficient C_d with sufficient accuracy to obtain reasonable Nytrox massflow results. These tests were performed using the Batch 2 Nytrox mixture. A total of 10 cold-flow calibration runs were performed, with the first 5 batches flowing for 2 seconds each and the last 5 flowing for 10 seconds each. The regulator pressure was set to 310 psig, and the oxidizer in the NOS run tank was weighed before and after each burn. The cold flow test apparatus was identical to the previously- described hot flow setup, except that the thrust chamber and fuel grain were removed and the ignition spark was not initiated.

Figure 15 plots the cold-flow test results. Plotted are the test data, a linear least squares curve fit, and the curve uncertainties boundaries plotted at the 95% confidence level. The abscissa plots

Citation: Whitmore SA, Stoddard RL. N_2O/O_2 blends safe and volumetrically efficient oxidizers for small spacecraft hybrid propulsion. *Aeron Aero Open Access J.* 2019;3(4):171–196. DOI: 10.15406/aaoaj.2019.03.00097

the total integrated massflow over the cold-flow run as predicted by the compressible venturi model from Eqs. (1) and (2), assuming that C_d=1.0. The ordinate plots the actual flowed oxidizer mass measured from the pre-and post-test weights of the NOS run tank. The curve fit coefficients are also noted on this fit. Generally, the fit is rather good with only slight bias of about 2.6 grams, which is likely due to a tank tare weight error.

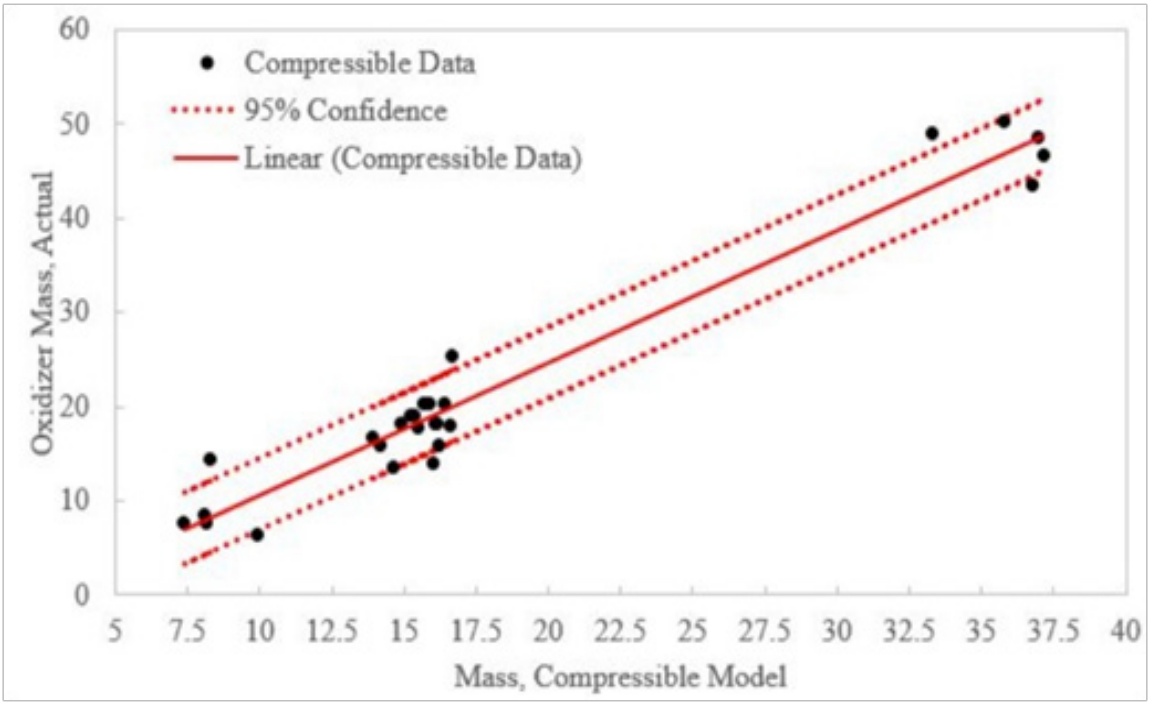

Figure 15 Nytrox Venturi calibration data.

Interestingly, the curve fit shows a slope (corresponding to the effective discharge coefficient) value at approximately 1.389; a value which is theoretically larger than the maximum possible value of 1.0 for an ideal gas flow. Clearly, there were some un-modeled two-phase effects happening during this flow. With this method the molecular weight, gas constant, and ratio specific heats were calculated based on the tank ullage vapor composition as shown by Table 2, with being calculated from the averages of the two Nytrox batches. Pressing forward to the Nytrox Hot-fire testing campaign the following parameters were used for the venturi flow calibration,

- $M_W = 38.625\ g/mol$
- $\gamma = 1.3399$
- $R_g = 215.26\ J/kg{-}K$
- $C_d = 1.38915$

Baseline GOX hot fire test summary

As stated previously, a series of hot fire test with GOX as the oxidizer were performed in order to establish a baseline for the small thruster system. Figure 16 summarizes the baseline test results. Plotted are I_{sp}, C_F, c^*, and the mean ABS fuel regression rate. The fuel regression rate is plotted as a function of both oxidizer G_{ox} and total massflux G_{total}. Because the achieved *O/F* ratio for the GOX/ABS thruster is rather low, Figure 18(d) demonstrates clearly that the ablated fuel massflux has a considerable effect on the overall fuel regression rate. The specific impulse and thrust coefficient curves plot values calculated using both the sensed thrust from the load cell, and the thrust calculated from chamber pressure using the method described in the previous section. The expected values calculated from CEA[24] assuming 100% combustion efficiency and frozen flow at the nozzle throat. are also overlaid on the are I_{sp}, C_F and c^* plots. The plotted data are generally supported by the theoretical calculations. Additionally, the values shown by Figure 16 agree with results previously published by refs. Refs,[7,8] and these results support the hypothesis that the reassembled test article and test stand was returned to its previous state of performance, for which there is an extensive data base.

Nytrox87 hot fire test summary

Figure 17 summarizes the results of the 10 Nytrox hot fire tests. The Nytrox mixtures used for these tests are described previously, with the mixture properties listed by Table 2. As with the previous plot of the baseline data, Figure 17 plots I_{sp}, C_F, c^*, and the mean ABS fuel regression rate plotted as a function of both G_{ox} and G_{total}. Note that, due to the higher *O/F* ratio, the ablated fuel massflux has a lower overall influence upon the fuel regression rate. The corresponding CEA curves assuming a *Nytrox 87* (87% N_2O) liquid composition are also plotted. Here there is significantly more scatter exhibited by the data, a likely result of the massflow uncertainty as calculated by the venturi flow meter, and the variability of the Nytrox fluid composition as the tank empties. As expected from the theoretical comparisons of Figure 9 the mean I_{sp} and c^* values are approximately 10% lower, due to the reduced flame temperature associated with Nytrox combustion. Also note that, when using Nytrox as a "drop in"

replacement for GOX, the motor tends to run slightly richer than the *O/F* value required for optimal performance. Since the thruster fuel grain had been previously optimized for best *O/F* ratio based on GOX as the oxidizer, this result is also not surprising. The mean Nytrox combustion efficiency, calculated for each burn as the ratio of the measured *c** to the theoretical value as predicted by CEA was 97.25%.

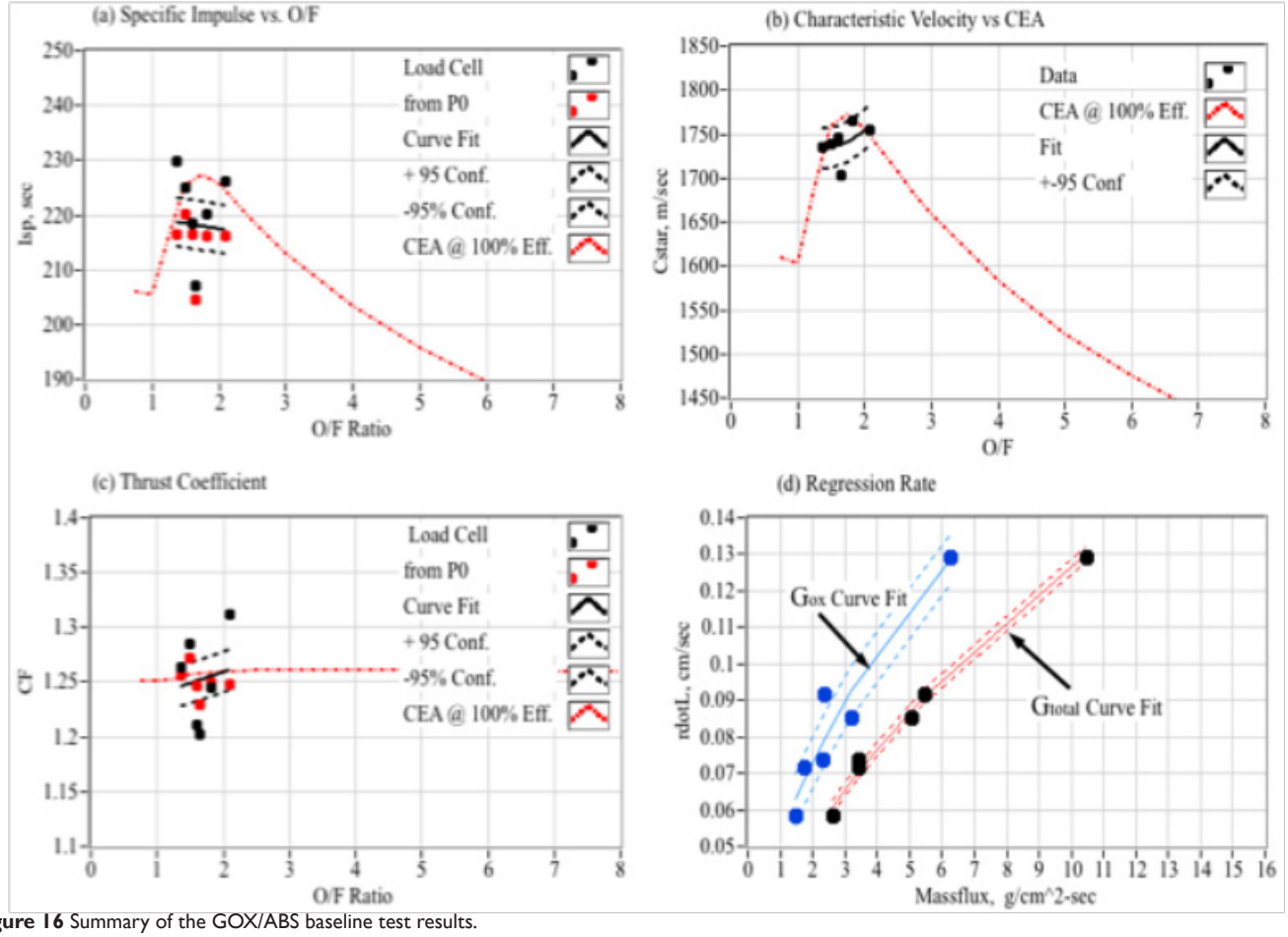

Figure 16 Summary of the GOX/ABS baseline test results.

Data comparisons

This section presents a series of bar charts that compare the mean properties of the thruster as derived from the 6 baseline and 10 Nytrox-evaluation hot fire tests. The comparisons include the nominal performance parameters I_{sp}, c^*, C_F, and $\rho^* I_{sp}$. Chamber pressure, mass flow mean oxidizer-to fuel-ratios and equivalence ratios are also compared. Their effects on fuel regression rate will be assessed. Finally, the required ignition energy, ignition reliability, and ignition latencies will be assessed and compared.

Performance comparisons

These bar charts compare the mean results from the hot fire test data presented in the previous section. Figure 18 compares the mean performance parameters including I_{sp}, c^*, and C_F, along with the mean operating chamber pressure P_0 and mass flows of the thruster using the two propellant classes. The comparisons also show the error bars calculated assuming a student-t distribution and an 95% confidence level. As shown by Figures 18(a) & 18(b) the GOX/ABS data exhibit higher I_{sp} and c^* values, *224.4s* and *1740m/s*, respectively; than do the Nytrox/ABS data with I_{sp} and c^* values of *203.1s* and *1547m/s*, respectively. This result, as predicted by Figure 9(c), was expected. As shown by Figure 18(c) both propellant combination exhibit nearly identical thrust coefficient values, indicating that the nozzle geometry is well optimized for both test series.

Figure 18(d) compares the mean combustion chamber pressures. The GOX/ABS thruster system was originally tuned to achieve a design chamber pressure was approximately 830 kPa (120 psi). The Nytrox/ABS thruster was tuned to give the same thrust and chamber pressure level as the GOX/ABS by manually adjusting the upstream regular's manual output setting during the initial test firing, and before the evaluation burn series. Thus, both thruster systems achieved the design pressure level and thrust (10 N) rather precisely, indicating little nozzle erosion during the testing campaign. This chamber pressure equivalence is also reflected by the C_F bar-charts of Figure 18(c).

As shown by Figures 18(c), 18(d) & 18(e), it is also interesting to note that although both systems obtained nearly equivalent mechanical performance levels in terms of thrust and chamber pressure, the oxidizer and total massflow levels are entirely different.

Citation: Whitmore SA, Stoddard RL. N_2O/O_2 blends safe and volumetrically efficient oxidizers for small spacecraft hybrid propulsion. *Aeron Aero Open Access J.* 2019;3(4):171–196. DOI: 10.15406/aaoaj.2019.03.00097

The nytrox flow through the injector is approximately 25% higher than the GOX flow for the same pressure level; whereas, the total massflow for the Nytrox/ABS is only 10% higher. This proportionally lower total massflow, and overall thrust level is primarily due to the lower combustion temperature, and the associated lower c^* of the Nytrox/ABS propellants, as compared to GOX/ABS. This result was previously predicted by the CEA data presented in Figure 9(b), and is reflected by the bar-graphs of Figure 20(b).

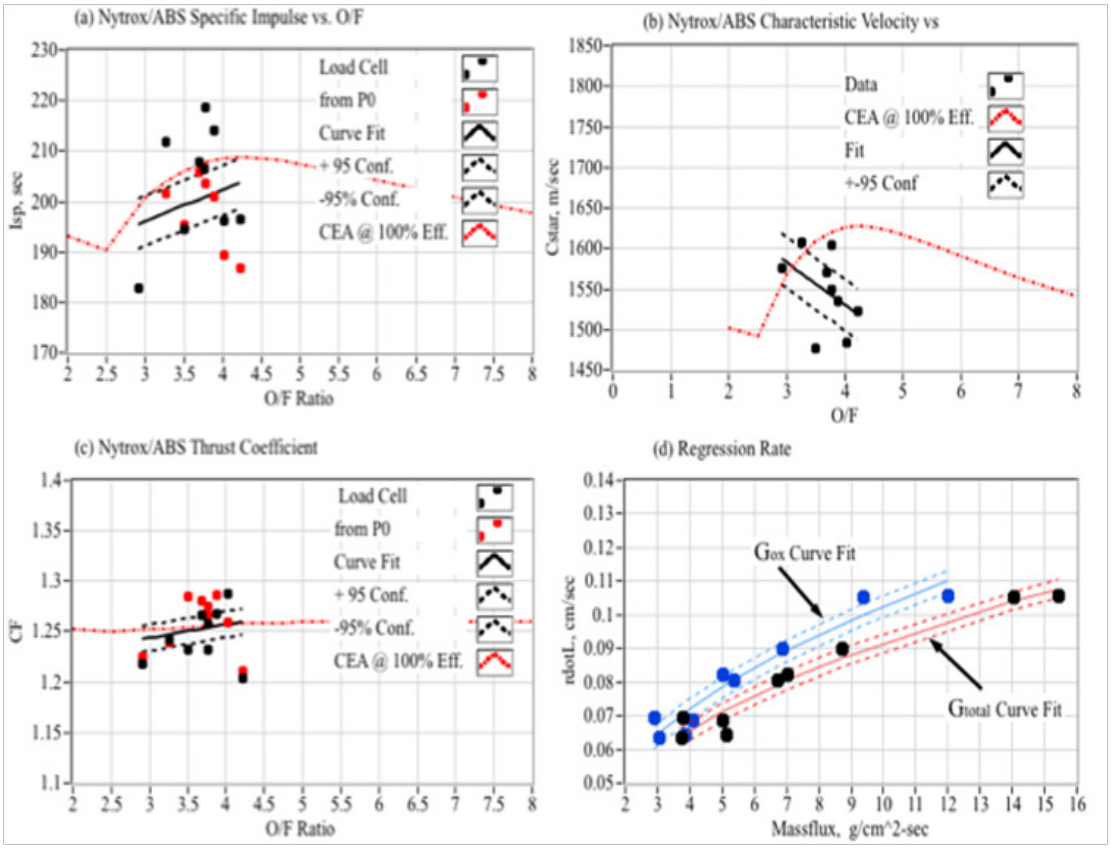

Figure 17 Summary of the Nytrox/ABS hot fire test results.

Figure 19 compares the mean density specific impulse values. In contrast to the mass-based I_{sp} comparisons, the *Nytrox/ABS* propellants exhibit a higher density specific impulse, approximately *1080 N-s/liter* compared to the *1036 N-s/liter* for *GOX/ABS* baseline. This calculation is based upon the oxidizer storage density, and not the downstream flow density. For this calculation the GOX is assumed to be stored at 2000 psig, and at 288ºC, with the resulting storage density of approximately *0.185g/cm³*. The Nytrox storage density is taken from the average of the two batches from Table 2 or approximately *0.423g/cm³*. Also, note that this relatively low Nytrox storage density results from the *NOS* run tank only being half-filled (5 lbs.) with nitrous oxide during processing. If the tank were filled to 3/4th capacity of 7.5 lbs. (3.4 kg), then the resulting storage density climbs to approximately, *0.562 g/cm³*, and the ρ^*I_{sp} value jumps to 1300 N-s/liter, and improvement of more nearly 23%. Figure 19(b) shows this result.

Oxidizer-to-fuel and equivalence ratio comparisons

Generally, ABS burned as a hybrid rocket fuel tends to have a higher overall performance when burned at an equivalence ratio F, the stoichiometric O/F divided by the actual O/F, which lies between 1.5 and 2.0. Burning at these fuel-rich equivalence ratios also has beneficial effect of reducing the flame temperature, lowering nozzle throat erosion, and producing a plume with a lower molecular weight composition.

The bar charts of Figure 20 compare the mean GOX/ABS and Nytrox87/ABS O/F and *Equivalence Ratios* from the hot-fire testing campaign. Figure 20(a) plots the mean O/F ratio for both GOX/ABS and Nytrox/ABS. Figure 20(a) also plots the theoretical stoichiometric O/F ratios. Figure 20(b) plots the equivalence ratios. Both fuels burn slightly rich, with the Nytrox/ABS burning richest. Note that although the O/F ratio increases significantly with the introduction of the higher density Nytrox as the oxidizer, the equivalence ratios for the two propellant combinations remain nearly constant, with only a slight increase in Φ for Nytrox/ABS. The GOX/ABS thruster was optimized to burn at an equivalence ratio of approximately 1.75, and the resulting O/F ratio tends to lie right on top of the O/F ratio for maximum c^*. Figure 20(b) shows this result. When GOX is swapped-out for NYtrox87; however, the resulting O/F ratio drops to a value slightly lower than the optimal level. Figure 20(b) shows the result. When burned with Nytrox, enlarging the initial port diameter of the ABS grain would shift the resulting O/F ratio back to near the optimal value, and presents a simple method for optimizing the fuel grain geometry.

Citation: Whitmore SA, Stoddard RL. N_2O/O_2 blends safe and volumetrically efficient oxidizers for small spacecraft hybrid propulsion. *Aeron Aero Open Access J.* 2019;3(4):171–196. DOI: 10.15406/aaoaj.2019.03.00097

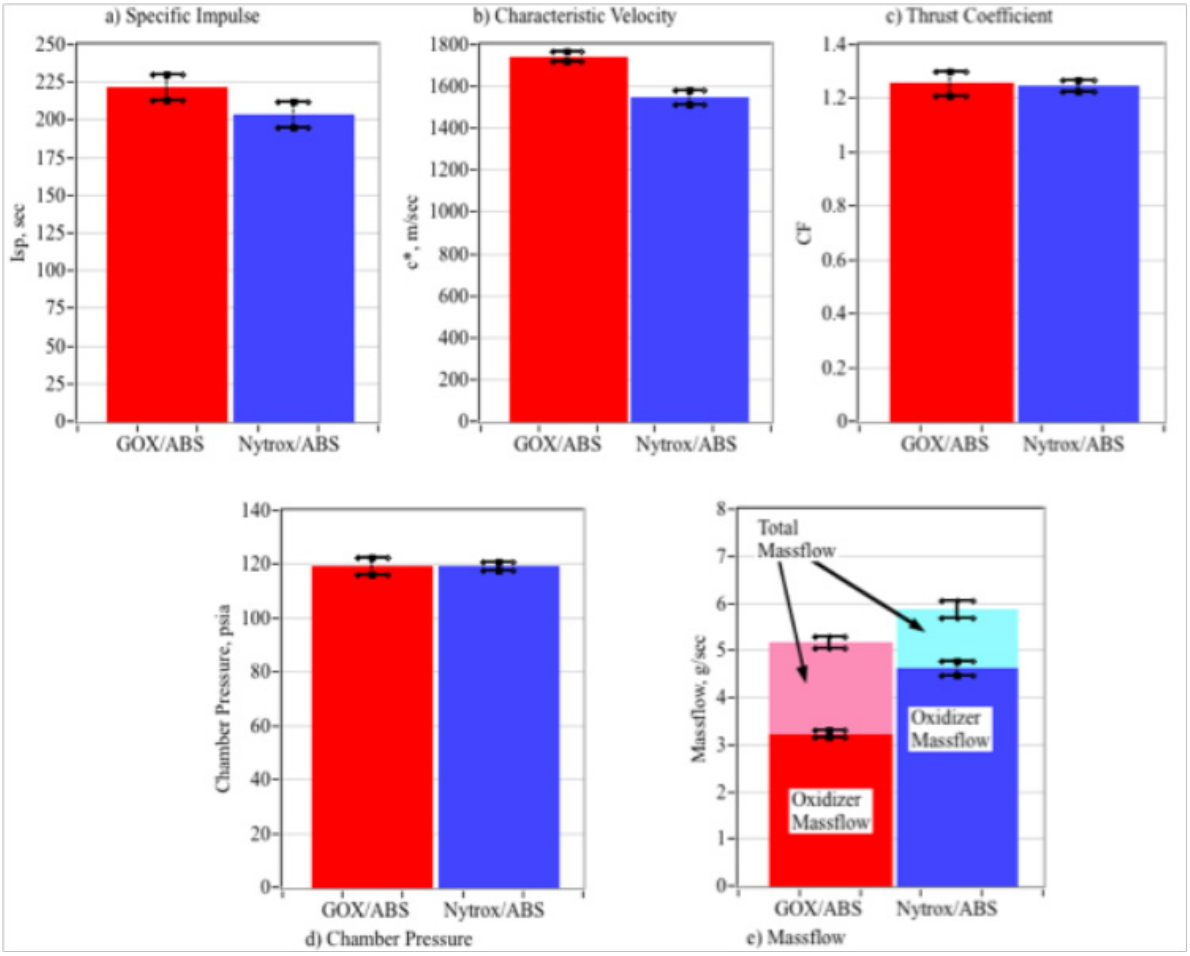

Figure 18 Comparing the performance of the test thruster using GOX/ABS and Nytrox87/ABS.

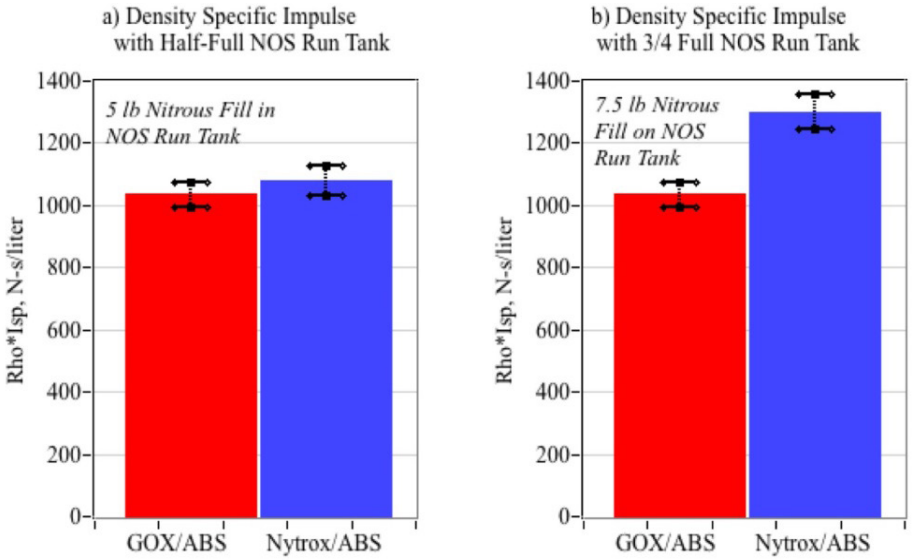

Figure 19 O/F and equivalence ratio comparisons.

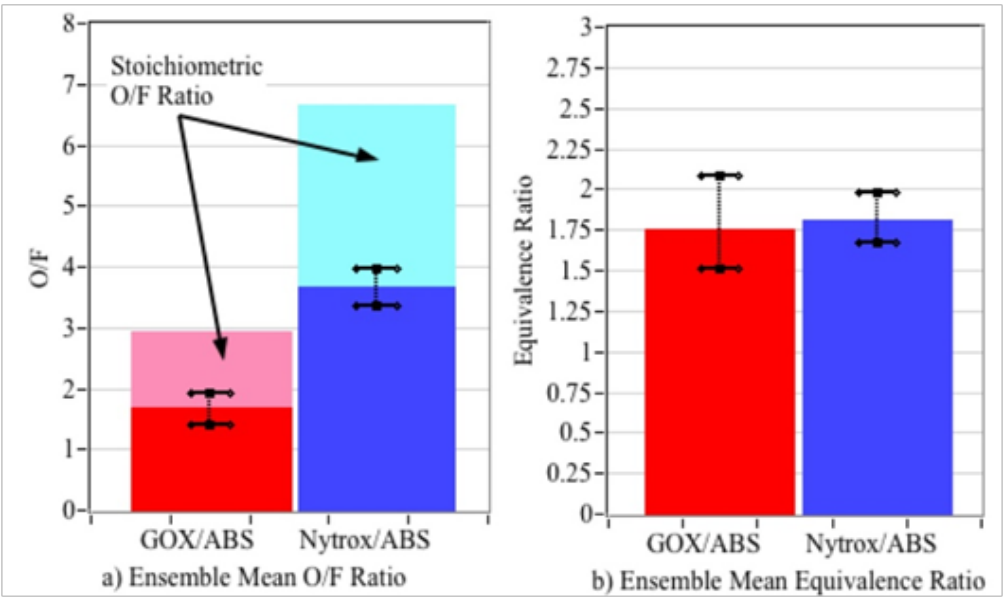

Figure 20 Comparing mean O/F and equivalence ratios for GOX/ABS and Nytrox87/ABS tests.

Fuel regression rate comparisons

Figure 21 compares the mean regression rates for GOX/ABS and Nytrox87/ABS. The Bar chart of Figure 21(a) compares the mean regression rates calculated by fitting the mean regression rate data of Figures 16(e) & 17(e) with an exponential curve fit of the form,

$$\dot{r} = a \cdot \bar{G}_{ox}^{n} \qquad (25)$$

and integrating over the operating massflux range, in this case *0-12 g/cm²-s*,

$$\bar{\dot{r}} = \frac{a}{G_{ox_{\max}}} \int_{0}^{G_{ox_{\max}}} \bar{G}_{ox}^{n} \cdot d\bar{G}_{ox} = \frac{a}{n+1} \cdot \bar{G}_{ox}^{n} \qquad (26)$$

Note that the GOX/ABS data exhibits a significantly higher regression rate then does Nytrox/ABS. Because essentially no database exists for the regression rates of fuels burned with Nytrox, the data of Figures 16(e) 17(e) are also overlaid with regression rate previously collected by the Author for a previous test campaign (Ref. [3]) at the PRL using Nitrous Oxide/HTPB and Nitrous/ABS as propellants. Also plotted are previously- derived[44] exponential curve fits for a) Liquid oxygen (LOX)/Paraffin, b) LOX/HTPB, c) N_2O/Escorez-HTPB, and d) LOX/High-density-polyethylene (HDPE). Table 3 summarizes the exponential fit parameters for the plotted curves on Figure 21(b). Although the regression rates achieved by GOX/ABS and LOX/Paraffin are clearly higher than the remainder of the propellant combinations; the Nytrox87/ABS regression rates are still clearly superior than N_2O as a stand-alone oxidizer, and is a factor that will lead to a smaller required fuel grain diameter. This volumetric reduction will partially offset the loss in overall system density that derives from the switch to Nytrox from N_2O.

Ignition reliability, latency, and required energy

As discussed previously, the arc-ignition system using GOX/ABS as propellants has been sufficiently matured to a power-efficient system that be started, stopped and restarted with a high degree of reliability. One of the key objectives of this research campaign was to demonstrate that Nytrox, can be "dropped in" to the system to significantly increase the volumetric efficiency of the propellants, while still allowing for a high degree of ignition reliability, with good energy efficiency. Clearly, the arc-ignition system was effective in igniting the Nytrox/ABS propellants; however, based on the data from the early testing campaign, the conclusions in this matter are somewhat mixed.

First, when a virgin fuel grain is first burned, the ignition reliability is less than 50% and pre-lead gaseous oxygen into the piping upstream of the run valve was required to ensure ignition. Once the first ignition is achieved, then the system reliably ignites with no GOX pre-lead, even with a dead-cold system. The reasons for this behavior are still unclear at this point in the development campaign, but the authors conjecture that the Nytrox expansion into the combustion chamber super-chills the fuel grain to the point that the ABS material impedance rises to a point where the HVPS cannot provide sufficient power to pyrolize the fuel grain. Once a conduction path is set into the fuel material after the initial burn, then this issue goes away. Cleary, further research is required in order to clearly determine the source of this behavior, and to establish procedures or methods that mitigate this difficulty for operational systems.

Second, the Nytrox/ABS propellants exhibit significantly higher ignition latencies compared to GOX/ABS. Figure 22 compares time histories demonstrating the typical ignition behavior for a 2-second pulse of the thruster system using first GOX/ABS, and then Nytrox 87/ABS. Plotted are (a) Thrust measured by the calibrated load cell, (b) Chamber Pressure, (c) Oxidizer massflow measured by the Venturi Flow meter, and (d) the Output ignition power from the HVPS. Note that for both runs the ignition power starts 1 full-second before the oxidizer run valve opens, and the ignition power profiles for both conditions are quite similar. After opening the oxidizer flow is immediate, and the GOX/ABS motor lights and reaches full operating

pressure within *200 milliseconds*. However, the Nytrox/ABS Motor exhibits a more significant latency, with an additional latency of approximately *250 ms* required to reach full chamber pressure. The authors believe that this latency is a result of super-chilled nytrox entering the combustion chamber, caused by the rapid expansion and phase change of the entering fluid. Not until the chamber pressure build up to more than two atmospheres does full ignition occurs. This two-atmosphere prerequisite for ignition was previously noted by Ref.[1]

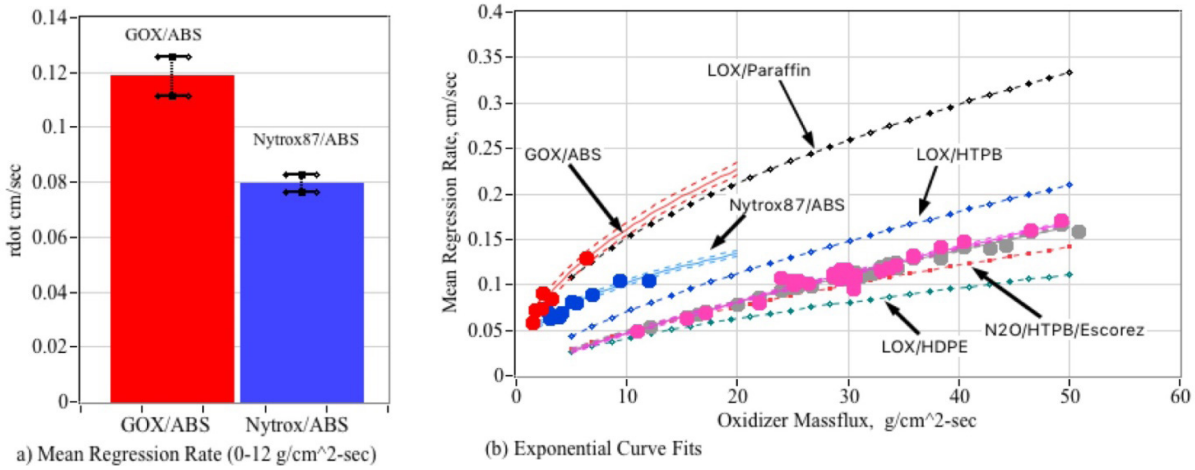

Figure 21 Regression rate comparisons.

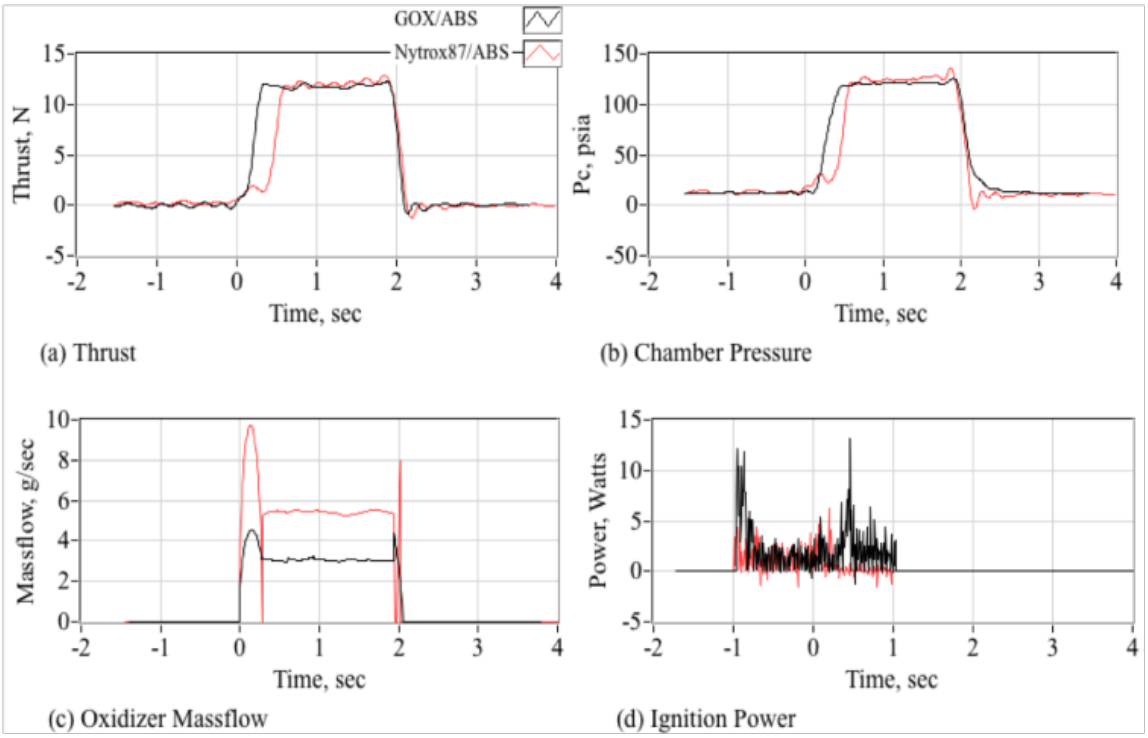

Figure 22 Comparisons of typical ignition response time histories for GOX/ABS and Nytrox87/ABS thrusters.

Table 3 Exponential fit parameters for GOX/ABS, Nytrox87/BS and other selected propellant regression rates

Propellant	GOX/ABS	Nytrox87/ABS	N_2O/ABS	N_2O/ HTPB	Paraffin/ LOX	LOX/ HTPB	Lox/HTPB-Escorez	LOX/HDPE
a coefficient	0.0522	0.04206	0.00742	0.00795	0.0488	0.0146	0.0099	0.0098
n exponent	0.491	0.387	0.799	0.773	0.491	0.681	0.68	0.62

Citation: Whitmore SA, Stoddard RL. N_2O/O_2 blends safe and volumetrically efficient oxidizers for small spacecraft hybrid propulsion. *Aeron Aero Open Access J.* 2019;3(4):171–196. DOI: 10.15406/aaoaj.2019.03.00097

The latency exhibited by the Nitrox/ABS thruster occurred for the entire test runs, and appears to be endemic to the use of Nytrox as a hybrid oxidizer. This latency can most likely only be overcome by the introduction of a catalyst material to jumpstart decomposition process and warm the flow upstream of the injector. Whitmore et al.,[45] have previously demonstrated the ability to significantly reduce arc-ignition combustion latencies with an upstream catalyst using 90% hydrogen peroxide and ABS propellants. Nytrox response latencies have not fully characterized at this point been, and are recommended as a point of emphasis for further study.

The bar chart of Figure 23 compares the required ignition energies for GOX/ABS and *Nytrox 87/ABS*. These data were calculated from the previously described data presented in Figures 16 and 17. Both propellant exhibit a very low required ignition energy, and in spite of the previously described ignition latency, the Nytrox/ABS propellants do not appear to need a statistically significantly great energy for startup. Both systems have a mean startup energy less than 3.5 joules, and to a 95% confidence level, neither require more than 5 joules for ignition. This energy level is contrasted to the ECAPS Prisma spacecraft[46] which used the ADN-based LMP-103s green propellant. For first ignition this system required a 10 watt preheat for as long as 20, consuming more than 12,000 joules of energy.

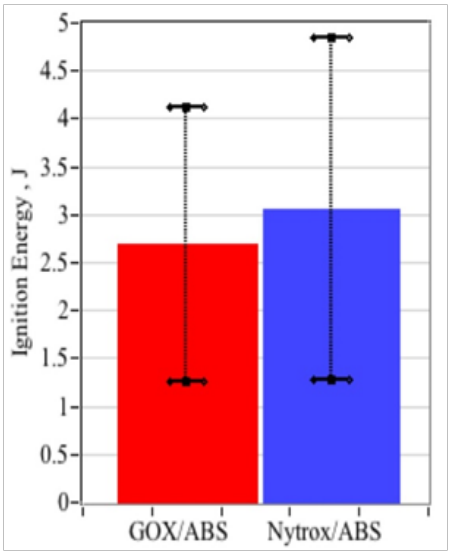

Figure 23 Comparing the required ignition energies for GOX/ABS and Nytrox87/ABS.

Effect of storage pressure and temperature on ignition latency

In a typical test-procedure the tank was chilled to zero C in an ice bath while filling, and then gradually warmed to ambient temperature during testing. An interesting result of this test procedure is that a clear correlation of the ignition latency to the tank storage temperature and pressure appeared. Figure 24 shows this result by plotting the ignition latency, calculated as the 63.2% first-order response rise time, plotted against the internal tank temperature. The trend is very distinctive with the latency growing from only 50 msec at the original pressure and temperature, to greater than 1 second as the tank warmed to room temperature.

It appears that, as the tank warms and the pressure level grows, then the saturated oxygen in solution begins to precipitate out. As the tank warms, the liquid Nytrox state has lesser and lesser oxygen in solution, making ignition increasingly more difficult to ignite. Thus, maintaining a cold tank temperature during firing appears to be an essential element to reducing ignition latency

The results plotted by Figure 25 support this assertion. Figure plots the oxygen mass-fraction in the nitrox solution using the previously discussed Peng-Robinson Model.[35] This calculation assumes that the tank is filled at 0ºC and 900 psi gauge pressure, with O_2 percolated to full saturation. The tank is subsequently warmed, allowing the internal pressure to rise, and also changing the mass proportions of O_2 in the vapor and liquid phases. The oxygen content in the liquid solution drops precipitously until at around 1100 psig internal pressure, the liquid phase become 100% nitrous oxide. This result was discovered shortly before the publication of this paper, and has not been fully explored. Clearly, a dedicated experiment with a direct measurement of the internal tank fluid temperature is required to reduce the data scatter. Wider pressure and temperature ranges, and initial saturation levels should also be explored. When fully comprehended, it appears that this method may result in engineering practices that reduce or fully eliminate the observed ignition latencies using the Nytrox oxidizer.

Extrapolating the specific impulse to vacuum conditions for Nytrox 87/ABS

Recall that the specific impulse and density-impulse values plotted on Figure 18 were derived from data collected under ambient test conditions at approximately 4700 ft. (1,430 meters) altitude, the elevation of the PRL test facility in Logan Utah. The 2.07 expansion-ratio nozzle was roughly design to give optimal performance at this altitude. Clearly, when matched with a high expansion-ratio nozzle, the vacuum performance will be significantly better. This data can be extrapolated to altitude by using the previously presented 1-D de Laval flow equations from Eqs. (16)-(24). Using this model, the specific impulse under optimal conditions can be written in terms of the optimal thrust coefficient and the nozzle exit-to-chamber pressure ratio. The result for thrust coefficient is

$$\left(C_{F_{vac}}\right)_{test} = \gamma \cdot \sqrt{\frac{2}{\gamma-1}\left(\frac{2}{\gamma+1}\right)^{\frac{\gamma+1}{\gamma-1}} \cdot \left(1-\frac{p_{exit}}{P_0}\right)^{\frac{\gamma-1}{\gamma}}} + \frac{A_{exit}}{A^*}\left(\frac{p_{exit}-p_\infty}{P_0}\right)$$

$$\left(C_{F_{vac}}\right)_{opt} = \gamma \cdot \sqrt{\frac{2}{\gamma-1}\left(\frac{2}{\gamma+1}\right)^{\frac{\gamma+1}{\gamma-1}} \cdot \left(1-\frac{p_\infty}{P_0}\right)^{\frac{\gamma-1}{\gamma}}} \tag{27}$$

Using CF to scale specific impulse,

$$\frac{\left(I_{sp}\right)_{opt}}{\left(I_{sp}\right)_{test}} = \frac{\frac{P_0 \cdot A^*}{g_0 \cdot \dot{m}}\left(C_{F_{opt}}\right)}{\frac{P_0 \cdot A^*}{g_0 \cdot \dot{m}}\left(C_{F_{test}}\right)} = \frac{\gamma \cdot \sqrt{\frac{2}{\gamma-1}\left(\frac{2}{\gamma+1}\right)^{\frac{\gamma+1}{\gamma-1}} \cdot \left(1-\left(\frac{(p_\infty)_{vac}}{P_0}\right)^{\frac{\gamma-1}{\gamma}}\right)}}{\gamma \cdot \sqrt{\frac{2}{\gamma-1}\left(\frac{2}{\gamma+1}\right)^{\frac{\gamma+1}{\gamma-1}} \cdot \left(1-\left(\frac{(p_\infty)_{vac}}{P_0}\right)^{\frac{\gamma-1}{\gamma}}\right)} + \left(\frac{A_{exit}}{A^*}\right)_{test} \cdot \left(\frac{(p_{exit})_{test}-p_\infty}{P_0}\right)} \tag{28}$$

Citation: Whitmore SA, Stoddard RL. N_2O/O_2 blends safe and volumetrically efficient oxidizers for small spacecraft hybrid propulsion. *Aeron Aero Open Access J.* 2019;3(4):171–196. DOI: 10.15406/aaoaj.2019.03.00097

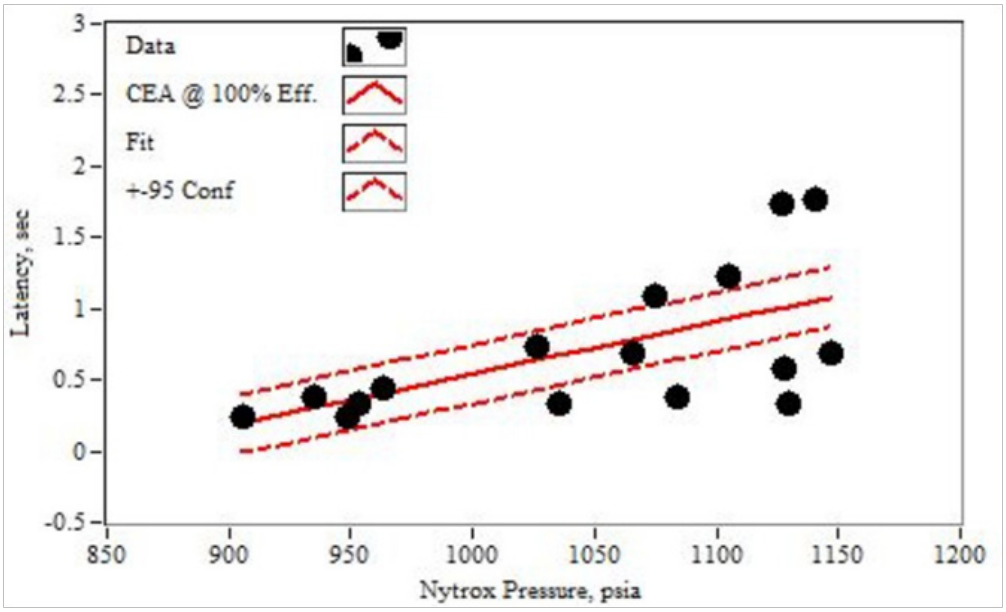

Figure 24 Thruster ignition latency correlated with internal Nytrox tank pressure.

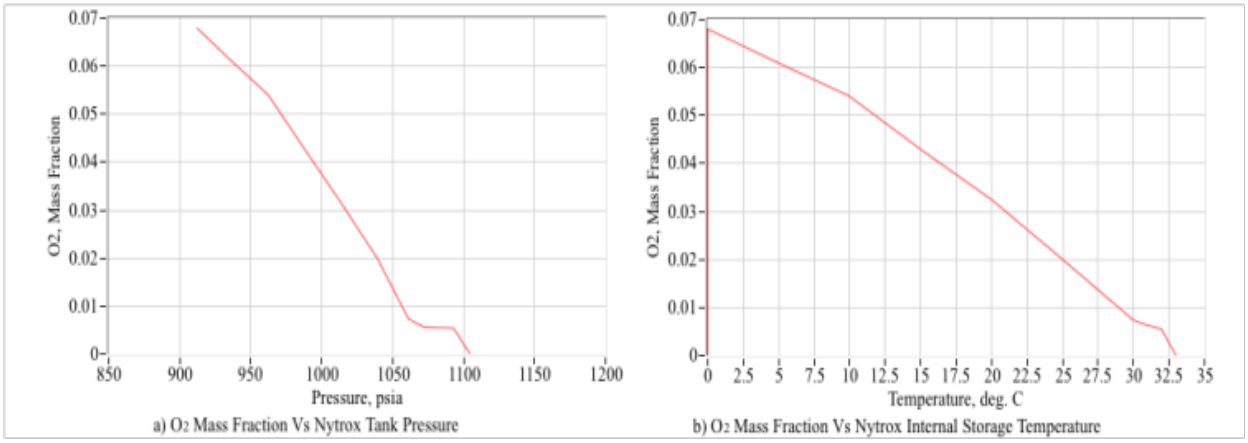

Figure 25 Peng-Robinson model prediction of O_2 mass faction in Nytrox liquid phase as function of tank temperature and pressure.

Using the motor parameters, thrust coefficient, mean chamber pressure, and the CEA-derived Thermochemistry

Parameters for *Nytrox 87*/ABS, and assuming a 97.3% combustion efficiency (from Section O., Figure 26 plots this extrapolation for both GOX and Nytrox oxidizers. Plotted are (a) optimal expansion ratio for the *Nytrox 87*/ABS motor as a function, (b) optimal CF as a function of expansion ratio, (c) optimal specific impulse as a function of expansion ratio, and (4) optimal specific impulse as a function of altitude. Also plotted as the red symbols are the actual values for the *Nytrox 87*/ABS motor. Note at an expansion ratio of 50, corresponding to an altitude of 29 km (95,000 ft.) the optimal C_F exceeds 1.8 and the optimal I_{sp} reaches a value of approximately *295 s*. This I_{sp} value is more than 25% higher than can be achieved by any of the "green" ionic liquid propellants or mono-propellant hydrazine. Using the *295s* I_{sp} value to extrapolate the ρ^*I_{sp} from Figure 21(b), the projected vacuum value rises to approximately *2560 N-s/liter*.

With more than 10 successful ground test burns, reliable on-demand ignitions have been demonstrated using *Nytrox 87* as a drop-in replacement for GOX in the USU Arc-ignition thruster system. Specific impulse values exceeding *200 s* under lab conditions have been demonstrated. This I_{sp} level extrapolates to nearly *300 s* under vacuum conditions with an optimized nozzle. This I_{sp} value far exceeds specific impulse values achieved by other available in-space monopropellants including hydrazine, LMP-103S, and AFM315-E. Table 4 compares the performance of the peroxide/ABS system to hydrazine, LMP-103S and AFM315-E.[47] With the exception of ρ^*I_{sp}, the Nytrox/ABS system outperforms the other propellants in every measureable category. However, even this lower density I_{sp} value is misleading. Because Nytrox had the ability to safely self-pressurize, there is no need for an additional volumetrically inefficient to safely self-pressurize, there is no need for an additional volumetrically inefficient oxidizer pressurization system. Thus, even in terms of volumetric efficiency, *Nytrox 87*/ABS appears to have a clear advantage.

Citation: Whitmore SA, Stoddard RL. N_2O/O_2 blends safe and volumetrically efficient oxidizers for small spacecraft hybrid propulsion. *Aeron Aero Open Access J.* 2019;3(4):171–196. DOI: 10.15406/aaoaj.2019.03.00097

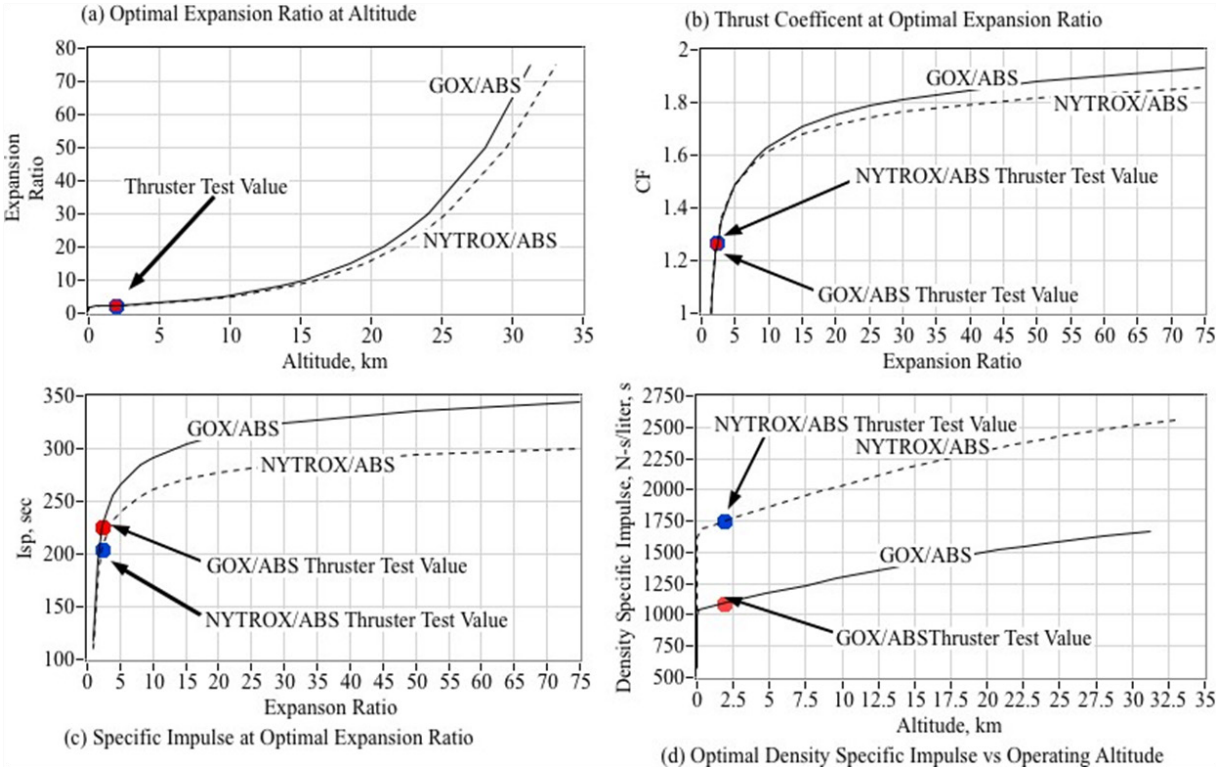

Figure 26 Extrapolating test specific impulse and thrust coefficient to optimal high altitude conditions.

Table 4 Comparison of Nytrox/ABS performance characteristics to existing space mono-propellants[8]

Propellant	Hydrazine	LMP-103S	AF-M315E	Nytrox/ABS Hybrid
Flame Temperature	600-750°C	1600°C	1900°C	3000°C[1]
I_{sp}, s	220-225	252 (theory),	266 (theory)	300 (theory)
		235 (delivered)	245 (delivered)	294 (delivered)[2]
Specific Gravity	1.01	1.24	1.465	0.650 (87% N_2O)
Density Impulse, *N-s/liter*	2270	3125 (theory)	3900(theory)	2560 (vacuum, extrapolated)
		2915 (delivered)	3650 (delivered)	1900 (ambient, delivered)
Preheat Temperature	315°C, cold-start capable	300°C	370°C	N/A none-required
Required Ignition Input Energy, *Joules*	N/A	12,000 J (10 Watts @ 1200 seconds)	27,000 J (15 Watts @ 1800 seconds	2-5 J (4-10 Watts for 500 msec)
Propellant Freezing Temperature	1-2°C	-7°C	< 0°C (*forms glass, no freezing point*)	-70°C
Cost	$	$$$	$$$$	$
Availability	Readily Available	Restricted Access	Limited Access	Very Widely Available[3]
NFPA 704 Hazard Class			  [5]	

[1]Data for hydrazine, LMP-103S and AFM315-E were taken from Ref. [7].

[2]Due to the high pyrolysis energy of ABS fuel, 3.1 MJ/kg, motors are ablative and self-cooling.

[3]Extrapolated to vacuum conditions based on ground test data.

[4]80-90% N2O solutions easily manufactured, as per procedure in this paper.

[5]Based up the constituent components, Hydroxyl Ammonium Nitrate (HAN) and 2-Hydroxyethylhydrazine (HEHN)

Citation: Whitmore SA, Stoddard RL. N_2O/O_2 blends safe and volumetrically efficient oxidizers for small spacecraft hybrid propulsion. *Aeron Aero Open Access J.* 2019;3(4):171–196. DOI: 10.15406/aaoaj.2019.03.00097

Summary and conclusion

The Propulsion Research Laboratory (PRL) at Utah State University recently developed a promising "green" propulsion alternative that has the potential to replace hydrazine for multiple applications. The unique hybrid propulsion technology derives from the novel electrical breakdown properties of 3-D printed ABS discovered serendipitously while investigating the thermodynamic performance of ABS as a hybrid rocket fuel. This concept has been developed into a power-efficient system that can be started and restarted with a high degree of reliability. Multiple prototype ground-test units with thrust levels varying from 4.5 N to 900 N have been developed and tested.

This paper investigates the use of a medical grade nitrous oxide and gaseous oxygen fluid blend, "Nytrox," as an intrinsically safer alternative to both gaseous oxygen and pure nitrous oxide as a hybrid rocket oxidizer. In a manner directly analogous to the creation of soda-water using dissolved carbon oxide, Nytrox is created by bubbling gaseous oxygen under high pressure into nitrous oxide until the solution reaches saturation level. Oxygen in mixture ullage dilutes the nitrous oxide vapor, and increases the required decomposition activation energy of the fluid by several orders of magnitude. Consequently, any risk of inadvertent thermal or catalytic decomposition is virtually eliminated. This paper reports on a preliminary test-and-evaluation campaign where an existing small spacecraft thruster is first tested using gaseous oxygen and 3-D printed ABS as propellants as a baseline.

A simple percolation procedure for manufacturing an 87% Nytrox solution using high-purity, medical grade nitrous oxide and gaseous oxygen was developed and reported. At this reporting two 6.5 liter batches of Nytrox have been prepared using the reported procedure. Both batches were remarkably consistent, agreeing well with theoretical predictions for density and saturation pressure. With more than 10 successful ground test burns, reliable on-demand ignitions have been demonstrated using Nytrox 87 as a drop-in replacement for GOX in the USU Arc-ignition thruster system. Clearly, the arc ignition system was effective in igniting the Nytrox/ABS propellants; with no statistically significant increase in the overall ignition energy requirements. However, based on the data from the early testing campaign, the conclusions in this matter are somewhat mixed.

First, when a virgin fuel grain is first burned, the ignition reliability is less than 50% and pre-lead gaseous oxygen into the piping upstream of the run valve was required to ensure ignition. Once the first ignition is achieved, then the system reliably ignites with no GOX pre-lead, even with a dead-cold system. The reasons for this behavior are still unclear at this point in the development campaign, but the authors conjecture that the Nytrox expansion into the combustion chamber super-chills the fuel grain to the point that the ABS material impedance rises to a point where the HVPS cannot provide sufficient power to pyrolize the fuel grain. Once a conduction path is set into the fuel material after the initial burn, then this issue goes away.

Second, the Nytrox/ABS propellants exhibit significantly higher ignition latencies compared to GOX/ABS. However, the Nytrox/ABS Motor exhibits a more significant latency, with an additional latency of approximately *250 ms* required to reach full chamber pressure. The authors believe that this latency is a result of super-chilled nytrox entering the combustion chamber, caused by the rapid expansion and phase change of the entering fluid. Not until the chamber pressure build up to more than two atmospheres does full ignition occurs. The latency exhibited by the Nitrox/ABS thruster occurred for the entire test runs, and appears to be endemic to the use of Nytrox as a hybrid oxidizer. This latency can most likely only be overcome by the introduction of a catalyst material to jumpstart decomposition process and warm the flow upstream of the injector. Nytrox response latencies have not fully characterized at this point been, and are recommended as a point of emphasis for further study.

It appears that, as the tank warms and the pressure level grows, then the saturated oxygen in solution begins to precipitate out. As the tank warms, the liquid Nytrox state has lesser and lesser oxygen in solution, making ignition increasingly more difficult to ignite. Thus, maintaining a cold tank temperature during firing appears to be an essential element to reducing ignition latency. This result was discovered shortly before the publication of this paper, and has not been fully explored. This discovery may result in engineering practices that reduce or fully eliminate the observed ignition latencies using the Nytrox oxidizer.

Finally, specific impulse values exceeding *200 s* under lab conditions have been demonstrated. This I_{sp} level extrapolates to nearly *300 s* under vacuum conditions with an optimized nozzle. This I_{sp} value far exceeds specific impulse values achieved by other available in-space monopropellants including hydrazine, LMP-103S,

and AFM315-E. With the exception of density specific impulse, the Nytrox/ABS system outperforms the other propellants in every measureable category. However, even this lower density I_{sp} value is misleading; because Nytrox had the ability to safely self-pressurize, there is no need for an additional volumetrically inefficient oxidizer pressurization system. Thus, even in terms of volumetric efficiency, *Nytrox 87*/ABS appears to have a clear advantage. When fully developed, a Nytrox-based hybrid system offers high value to the commercial space industry by offering a high-performing, but inherently safe, space propulsion option for rideshare payloads.

Patents

Whitmore SA. Restartable Ignition Devices, Systems, and Methods Thereof. USA Provisional Patent No. US 2015/A0322892 A1, Nov. 12, 2015.

Funding

This work was partially funded with a cooperative agreement with the NASA Marshall Spaceflight Center, Cooperative Agreement No. NNM16AA01A.

Acknowledgments

The author is especially grateful for the assistance of NASA Marshall Space Flight Center (MSFC) ER-23, by graciously provided access to the testing facilities used to collect vacuum chamber data for this project. I deeply appreciate MSFC employees Kevin Pedersen, Carlos Diaz, and Daniel Cavender for their time, technical support, and expert advice.

Conflicts of interest

The authors declare no conflict of interest.

Citation: Whitmore SA, Stoddard RL. N_2O/O_2 blends safe and volumetrically efficient oxidizers for small spacecraft hybrid propulsion. *Aeron Aero Open Access J.* 2019;3(4):171–196. DOI: 10.15406/aaoaj.2019.03.00097

References

1. Whitmore SA, Inkley NR, Merkley DP, et al. Development of a Power-Efficient, Restart-Capable Arc Ignitor for Hybrid Rockets. Journal of Propulsion and Power. 2015;31(6):1739–1749.
2. Whitmore SA. Additively Manufactured Acrylonitrile-Butadiene-Styrene–Nitrous-Oxide Hybrid Rocket Motor with Electrostatic Igniter. *J Propulsion Power*. 2015;31(4):1217–1220.
3. Whitmore SA, Peterson ZW, Eilers SD. Comparing Hydroxyl Terminated Polybutadiene and Acrylonitrile Butadiene Styrene as Hybrid Rocket Fuels. *J Propulsion Power*. 2013;29(3):582–592.
4. Whitmore SA. *Additive Manufacturing as an Enabling Technology for "Green" Hybrid Spacecraft Propulsion*. Conference on Recent Advances in Space Technology 2015: Istanbul, Turkey; 2015.
5. Whitmore SA, Merkley SL, Zachary S, et al. *Development of a Power Efficient, Restartable, "Green" Propellant Thruster for Small Spacecraft and Satellites*. SSC15-P-34, 29th AIAA/USU Conference on Small Satellites: Logan, UT; 2015.
6. Whitmore SA, Bulcher AM. *A Green Hybrid Thruster Using Moderately Enriched Compressed Air as the Oxidizer*. 2018 Joint Propulsion Conference, AIAA Propulsion and Energy Forum; 2018.
7. Whitmore SA, Bulcher AM. *Vacuum Test of a Novel Green-Propellant Thruster for Small Spacecraft*. AIAA 2017-5044. 53rd AIAA/SAE/ASEE Joint Propulsion Conference, AIAA Propulsion and Energy Forum; 2017.
8. Whitmore SA. Three-Dimensional Printing of "Green" Fuels for Low-Cost Small Spacecraft Propulsion Systems. *Journal of Spacecraft and Rockets*. 2017;54(6):337–382.
9. Bombelli V. *Economic Benefits for the Use of Non-toxic Monopropellants for Spacecraft Applications*. AIAA-2003-4783, 39th AIAA/ASME/SAE/ASEE Joint Propulsion Conference and Exhibit: Huntsville, AL; 2003.
10. Haeseler D, Bombelli V, Vuillermoz P, et al. *Green Propellant Propulsion Concepts for Space Transportation and Technology Development Needs*. ESA SP-557, Proceedings of the 2nd International Conference on Green Propellants for Space Propulsion: Cagliari, Sardinia, Italy; 2004.
11. Goldstein E. *The Greening of Satellite Propulsion*. Aerospace America; 2012. 26–28 p.
12. Venkatachalam S, Santhosh G, Ninan KN. An Overview on the Synthetic Routes and Properties of Ammonium Dinitramide (ADN) and other Dinitramide Salts. *J Propellants, Explosives, Pyrotechnics*. 2004;29(3):178–187.
13. Nagamachi MY, Oliveira JI, Kawamoto AM, et al. ADN–The new oxidizer around the corner for an environmentally friendly smokeless propellant. *J Aerospace Technology Management*. 2009;1(2):153–160.
14. Rheingold AL, Cronin JT, Brill TB, et al. Structure of Hydroxylammonium Nitrate (HAN) and the Deuterium Homolog. *Acta Crystallographica*. 1987;43(1):402–404.
15. Hawkins TW, Brand AJ, McKay MB, et al. *Reduced Toxicity, High performance Monopropellant at the U.S. Air Force Research Laboratory*. AFRL-RZ-ED-TP-2010-219, 4th International Association for the Advancement of Space Safety Conference: Huntsville, AL; 2010.
16. Persson M, Anflo K, Dinardi A. *A Family of Thrusters for ADN-Based Monopropellant LMP-103S*. AIAA-2012-3815, 48th AIAA/ASME/SAE/ASEE Joint Propulsion Conference & Exhibit: Atlanta, Georgia; 2012.
17. Spores RA, Masse R, Kimbrel S. *GPIM AF-M315E Propulsion System*. AIAA_2013-3849, 49th AIAA/ASME/SAE/ASEE Joint Propulsion Conference & Exhibit: San Jose CA; 2013.
18. Whitmore SA, Burnside CG. *Performance Analysis of a High Performance Green Propellant Thruster*. Proceedings of the NASA Marshall Space Flight Center Faculty Program, NASA TM-2015-218216; 2015. 125–151 p.
19. Anon. Hazard Analysis of Commercial Space Transportation; Vol. 1: Operations, Vol. 2: Hazards, vol. 3: Risk Analysis," U.S. Dept Transportation, PB93-199040, Accession No. 00620693; 1988.
20. Bond TA, Christensen JA. *NSTAR Ion Thrusters and Power Processors*. NASA/CR--1999-209162;1999.
21. Anon. Deep Space 1, Mission to Asteroid 9969 Braille, Comet Borrelly. JPL Web Link; 2018.
22. Anon. *Dawn at a Glance*. JPL Web Link; 2018.
23. Anon. Department of Defense Interface Standard, Eletromagnetic Environmental Effects requirements for Systems, MIL-STD-464; 2018.
24. Gordon S, McBride BJ. *Computer Program for Calculation of Complex Chemical Equilibrium Compositions and Applications*. NASA Technical Report RP-1311; 1994.
25. Whitmore SA, Armstrong IW, Heiner MC, et al. High-Performing Hydrogen Peroxide Hybrid Rocket with 3-D Printed and Extruded ABS Fuel. *Aeronautics and Aerospace Open Access Journal*. 2018;2(6):334–354.
26. Whitmore SA, Martinez CJ, Merkley DP. Catalyst Development for an Arc-Ignited Hydrogen Peroxide/ABS Hybrid Rocket System. *Aeronautics and Aerospace Open Access Journal*. 2018;2(6):356–388.
27. Rommingen JE, Husdal J. *Nammo Hybrid Rocket Propulsion TRL Improvement Program*. AIAA 2012-4311, 8th AIAA/ASME/SAE/ASEE Joint Propulsion Conference & Exhibit, Joint Propulsion Conferences; 2012.
28. Anthoine J, Jean-Yves Lestrade JY, Messineo J, et al. *Performances of a Multi-Pulsed Hybrid Rocket Engine Operating with Highly Concentrated Hydrogen Peroxide*. AIAA 2017-4006, 53rd AIAA/SAE/ASEE Joint Propulsion Conference, AIAA Propulsion and Energy Forum; 2017.
29. Whitmore SA. Direct Ignition of a High Performance Hydrogen Peroxide Hybrid Rocket with 3-D Printed Fuel. *Int J Astronautics Aeronautical Engineering*. 2019;4(1):1–22.
30. Anon. *Safety Standard for Oxygen and Oxygen Systems*. NSS 1740.15, NASA Office of Mission Assurance: Washington DC; 1996.
31. Anon. *Occupational Safety and Health Guideline for Nitrous Oxide*. US Department of Labor, Occupational Health and safety Administration; 2018.
32. Rhodes GW. *Investigation of Decomposition Characteristics of Gaseous and Liquid Nitrous Oxide*. Air Force Weapons Laboratory, Report AD-784 602, Kirtland AFB: New Mexico; 1974.

Citation: Whitmore SA, Stoddard RL. N_2O/O_2 blends safe and volumetrically efficient oxidizers for small spacecraft hybrid propulsion. *Aeron Aero Open Access J*. 2019;3(4):171–196. DOI: 10.15406/aaoaj.2019.03.00097

33. Karabeyoglu A, Dyer J, Stevens J, et al. *Modeling of N_2O Decomposition Events*. AIAA 2008-4933, 44th AIAA/ASME/SAE/ASEE Joint Propulsion Conference and Exhibit: Hartford CT; 2008.

34. Bracken AB, Broughton GB, Hill W. Equilibria for Mixtures of Oxygen and Nitrous Oxide and Carbon Dioxide and Their Relevance to the Storage of N2O/O2 Cylinders for Use in Analgesia. *Journal of Physics D*. 1970;3:1747–1758.

35. Karabeyoglu MA. Nitrous Oxide and Oxygen Mixtures (Nytrox) as Oxidizers for Rocket Propulsion Applications. *Journal of Propulsion and Power*. 2014;30(3):696–706.

36. Peng DY, Robinson DB. A New Two Constant Equation of State. *Industrial and Engineering Chemistry Fundamentals*. 1976;15(1):59–64.

37. Zudkevitch D, Joffe J. Correlation and Prediction of Vapor- Liquid Equilibria with the Redlich- Kwong Equation of State. *AIChE Journal*. 1970;16(1):112–119.

38. Anderson JD. *Modern Compressible Flow*. 3rd ed. New York: The McGraw Hill Companies, Inc.; 2003. 127–187 p.

39. Zilliac G, Karabeyoglu MA. *Modeling of Propellant Tank Pressurization*. AIAA 2005-3549, 41st AIAA/ASME/SAE/ASEE Joint Propulsion Conference & Exhibit: Tucson, Arizona; 2005. 1–25 p.

40. Dyer J, Doran E, Dunn Z, et al. *Modeling Feed System Flow Physics for Self-Pressuring Propellants*. 43rd AIAA/ASME/ SAE/ASEE Joint Propulsion Conference & Exhibit, AIAA Paper 2007- 5702; 2007.

41. Whitmore SA, Chandler SN. *Engineering Model for Self-Pressurizing Saturated-N_2O-Propellant Feed Systems*. J Propulsion and Power. 2010;26(4):706–714.

42. Zimmerman JE, Waxman BS, Cantwell BJ, et al. *Review and Evaluation of Models for Self-Pressurizing Propellant Tank Dynamics*. AIAA 2013-4045, 49th AIAA/ASME/SAE/ASEE Joint Propulsion Conference & Exhibit: San Jose CA; 2013.

43. Waxman BS, Zimmerman JE, Cantwell BJ, et al. *Mass Flow Rate Characterization of Injectors for Use with Self-Pressurizing Oxidizers in Hybrid Rockets*. 60th JANNAF Propulsion Meeting; 2013.

44. Zilliac G, Karabeyoglu MA. *Hybrid Rocket Fuel Regression Rate Data and Modeling*. AIAA Paper 2006-4504; 2006.

45. Whitmore SA, Martinez CJ, Merkley DP. Catalyst development for an arc-ignited hydrogen peroxide/ABS hybrid rocket system. *Aeronautics and Aerospace Open Access Journal*. 2018;2(6):356–388.

46. Persson M, Anflo K, Dinardi A. *A Family of Thrusters for ADN-Based Monopropellant LMP-103S*. AIAA-2012-3815, 48th AIAA/ASME/SAE/ASEE Joint Propulsion Conference & Exhibit: Atlanta, Georgia; 2012.

47. Brand AJ. *Reduced Toxicity High Performance Monopropellant*. AFRL-RZ-ED-VG-2011-326, Green Propellants Workshop: Stockholm, Sweden; 2011.